JBC Papers in Press. Published on December 18, 2018 as Manuscript RA118.004280
The latest version is at http://www.jbc.org/cgi/doi/10.1074/jbc.RA118.004280



# Combined treatment with the phenolics (−)-epigallocatechin-3-gallate and ferulic acid improves cognition and reduces Alzheimer-like pathology in mice

**Takashi Mori,[‡,§1] Naoki Koyama,[‡] Jun Tan,[‖,**] Tatsuya Segawa,[¶] Masahiro Maeda,[¶] and Terrence Town[‡‡2]**

*From the Departments of [‡]Biomedical Sciences and [§]Pathology, Saitama Medical Center and University, Kawagoe, Saitama 350-8550, Japan, the [‖]Rashid Laboratory for Developmental Neurobiology, Silver Child Development Center and the [**]Neuroimmunology Laboratory, Department of Psychiatry and Behavioral Neurosciences, Morsoni College of Medicine, University of South Florida, Tampa, Florida 33613, the [¶]Immuno-Biological Laboratories Co., Ltd., Fujioka, Gunma 375-0005, Japan, and the [‡‡]Zilkha Neurogenetic Institute, Department of Physiology and Biophysics, Keck School of Medicine, University of Southern California, Los Angeles, California 90089-2821*

Running title: *Combination therapy modifies Alzheimer-like pathology*

[1]To whom correspondence may be addressed: Depts. of Biomedical Sciences and Pathology, Saitama Medical Center and University, 1981 Kamoda, Kawagoe, Saitama 350-8550, Japan. Tel.: 81-49-228-3592; E-mail: t_mori@saitama-med.ac.jp.

[2]To whom correspondence may be addressed: Zilkha Neurogenetic Institute, Dept. of Physiology and Biophysics, Keck School of Medicine, University of Southern California, 1501 San Pablo St., Rm. 337, Los Angeles, CA 90089-2821. Tel.: 1-323-442-2492; E-mail: ttown@usc.edu

**Keywords:** Alzheimer's disease; α-secretase; amyloid β-protein; amyloid β-protein precursor; β-secretase; epigallocatechin-3-gallate; ferulic acid; nonamyloidogenic; phenol; plant; polyphenol

## Abstract

'Nutraceuticals' are well-tolerated natural dietary compounds with drug-like properties that make them attractive as Alzheimer's disease (AD) therapeutics. Combination therapy for AD has garnered attention following a recent National Institute on Aging mandate, but this approach has not yet been fully validated. In this report, we combined the two most promising nutraceuticals with complementary anti-amyloidogenic properties: the plant-derived phenolics (−)-epigallocatechin-3-gallate (EGCG, an α-secretase activator) and ferulic acid (FA, a β-secretase modulator). We used transgenic mice expressing mutant human amyloid β-protein precursor and presenilin 1 (APP/PS1) to model cerebral amyloidosis. At 12 months of age, we orally administered EGCG and/or FA (30 mg/kg each) or vehicle once daily for 3 months. At 15 months, combined EGCG-FA treatment reversed cognitive impairment in most tests of learning and memory, including novel object recognition and maze tasks. Moreover, EGCG- and FA-treated APP/PS1 mice exhibited amelioration of brain parenchymal and cerebral vascular β-amyloid deposits and decreased abundance of amyloid β-proteins compared with either EGCG or FA single treatment. Combined treatment elevated nonamyloidogenic soluble APP-α and α-secretase candidate and down-regulated amyloidogenic soluble APP-β, β-carboxyl-terminal APP fragment and β-secretase protein expression, providing evidence for a shift toward nonamyloidogenic APP processing. Additional beneficial co-treatment effects included amelioration of neuroinflammation, oxidative stress, and synaptotoxicity. Our findings offer preclinical evidence that combined



Downloaded from http://www.jbc.org/ by guest on January 9, 2019

treatment with EGCG and FA is a promising AD therapeutic approach.

---

Largely owed to significant increases in lifespan, Alzheimer's disease (AD) has become a worldwide public health concern. AD is a fatal neurodegenerative illness that likely begins with brain changes 20 years or more prior to clinical symptoms. AD is characterized by progressive decline in memory and other cognitive functions, eventually leading to dementia and death. Neuropathological hallmarks of AD include extracellular senile plaques and intracellular neurofibrillary tangles, accompanied by neuroinflammation, synaptic toxicity, and neuronal loss (1). Amyloid β-protein (Aβ)—a peptide derived from amyloid β-protein precursor (APP)—has garnered major interest as a therapeutic target for AD. Two enzymes, the β- and γ-secretases, cleave APP into smaller amyloidogenic peptides: $A\beta_{40}$ and $A\beta_{42}$, which can form both oligomeric and multimeric aggregates (2-5). Once cleaved from APP, Aβ enters into systemic equilibrium between its soluble and deposited forms (6). Conversely, nonamyloidogenic α-secretase cleavage of APP precludes Aβ formation and produces soluble APP-α (sAPP-α) (3, 7). Because the nonamyloidogenic pathway is the homeostatic default, this results in constitutively low Aβ levels.

Despite intense investigation, a synthetic drug that is both safe and effective has not yet been developed for AD. This inconvenient truth has led to the consideration of alternate strategies, including naturally occurring dietary compounds with therapeutic potential (so-called 'nutraceuticals'). Another important matter is a recent mandate to develop combination therapy for AD. Because nutraceuticals are generally safe and well-tolerated, these agents are more amenable to combination than designer drugs. In this report, we explore combination therapy with two promising nutraceuticals with complementary anti-amyloidogenic properties: (−)-epigallocatechin-3-gallate (EGCG, an α-secretase enhancer) (8, 9) and ferulic acid (FA, a β-secretase modulator) (10).

EGCG is a polyphenol catechin; the ester of epigallocatechin and gallic acid (11). EGCG is found in high abundance in tea leaves including green tea, and in carob flour (*i.e. Ceratonia siliqua*) at lesser abundance. Trace amounts are found in fruits (*e.g.* apple and cranberries) and nuts (*e.g.* pecans and hazelnuts) (12). EGCG has garnered attention as a medicinal agent to improve cognition, reduce inflammation, and even to treat cancer. Beneficial effects are often attributed to anti-oxidant, metal chelating, anti-inflammatory, anti-carcinogenic, and anti-apoptotic properties (13). Substantial quantities pass from the small to the large intestine, where EGCG undergoes degradation by gut flora and absorption. EGCG can be reabsorbed from the intestine through enterohepatic re-circulation (14, 15). It has been shown that dietary EGCG crosses the blood-brain barrier (16), and we were the first to show that EGCG enhances APP cleavage to sAPP-α and reduces Aβ abundance both in neuron-like cells and in Tg2576 mouse brains (8). A disintegrin and metalloproteinase domain-containing protein 10 (ADAM10) activation is mechanistically responsible for EGCG promotion of nonamyloidogenic α-secretase APP cleavage (9).

Like EGCG, FA is also a plant-derived compound. Seed plants and leaves (*e.g.* rice, wheat, and oats), vegetables (*e.g.* tomatoes and carrots), and fruits (*e.g.* pineapples and oranges) are the main sources of dietary FA. The compound has both anti-inflammatory and anti-oxidant properties (10, 17, 18), and we have previously shown that FA is a β-secretase modulator that inhibits amyloidogenic APP cleavage. We further reported that FA reverses cognitive/behavioral deficits and mitigates AD-like pathology after 6-months of oral treatment in the APP/PS1 transgenic mouse model of cerebral amyloidosis, and alters amyloidogenic β-



Downloaded from http://www.jbc.org/ by guest on January 9, 2019

secretase APP cleavage in mutant APP-overexpressing neuron-like cells (10). Because FA has a relatively low molecular weight, the compound is freely cell-permeable and bioavailable. FA is absorbed in free form via stomach mucosa, and then transported into the hepatic portal vein where it is metabolized in the liver. Of note, oral FA can be recovered in rat plasma after only 5 min, when the ratio of free FA to total FA is markedly increased, but rapidly gives rise to conjugated FA. Both free and conjugated FA are distributed via the systemic circulation (18-20). Both free and conjugated FA are distributed via the systemic circulation into peripheral tissues (19, 20). Whereas FA is negatively changed at physiological pH due to a hydroxyl moiety (21), the compound has been shown to cross the blood-brain barrier in rodents after peripheral administration (22, 23).

Given that both compounds share anti-inflammatory and anti-oxidant properties and have complementary modes of action on APP cleavage, we tested if combination therapy with EGCG and FA (each at 30 mg/kg) ameliorated learning and memory changes, cerebral amyloidosis, AD-like pathology, and amyloidogenic APP processing in the mutant human amyloid β-protein precursor-presenilin 1 (APP/PS1) transgenic mouse model of cerebral amyloidosis (APP/PS1 mice). We orally administered EGCG/FA (alone or in combination) or vehicle to APP/PS1 mice once daily for 3 months (beginning at 12 months of age), and evaluated animals at 15 months old. Here, our pre-clinical results show that combination therapy with EGCG plus FA has significant advantages over single treatment with either compound.

## Results

### *Co-treatment with EGCG and FA reverses learning and memory impairment in APP/PS1 mice*

APP/PS1 mice reportedly have transgene-related behavioral impairment as early as 5-7 months of age (24), so we began by assessing baseline cognitive status prior to dosing at 12 months. Data revealed behavioral impairment in novel object recognition, Y-maze, and radial arm water maze (RAWM) tests in our cohort of 12-month-old APP/PS1 mice *versus* wild-type (WT) littermate controls (data not shown). We then randomly assigned behaviorally impaired APP/PS1 mice (four treatments with $n = 8$ per group; equal numbers of four males and four females) and WT littermates (same group sizes and distribution as APP/PS1 mice). Single or double treatment (via gavage using a 6202 gastric tube with a rounded silicone-coated tip, FUCHIGAMI KIKAI, Kyoto, Japan) was given once daily for 3 months with EGCG and/or FA (each at 30 mg/kg) or vehicle beginning at 12 months in APP/PS1 and in WT littermate controls. This directly administered treatment more precisely derivers the targeted amount of agent compared with *ad libitum* access to drinking water or chow. At the end of treatment (15 months of age), we conducted a behavioral testing battery.

We initially assessed episodic memory by novel object recognition test, and all eight mouse groups showed similar recognition indices (50.3–52.5%) in the training phase of the test (Fig. 1*A*, *left*; Table S1). In the retention phase, one-way analysis of variance (ANOVA) followed by post hoc comparison disclosed statistically significant differences on recognition index between APP/PS1-V mice and the other seven mouse groups (Fig. 1*A*, r*ight*; Table S1; *, $p < 0.05$ for APP/PS1-V *versus* all other mouse groups). Singly- or doubly-treated APP/PS1 mice had significantly increased novel object exploration frequency by 60.8–71.6% *versus* APP/PS1-V mice (50.0%). Of note, EGCG/FA combination therapy completely mitigated episodic memory impairment (Fig. 1*A*, *right*; Table S1; †, $p < 0.05$, APP/PS1-EGCG/FA *versus* APP/PS1-EGCG or APP/PS1-FA mice), as there were no significant differences *versus* any of the WT mouse groups (Fig. 1*A*, *right*; Table S1; $p > 0.05$).



Downloaded from http://www.jbc.org/ by guest on January 9, 2019

We moved on to test exploratory activity and spatial working memory in the alternation Y-maze task. One-way ANOVA followed by post hoc testing revealed statistically significant differences for total arm entries between APP/PS1-V mice and the other seven mouse groups (Fig. 1*B*, *left*; Table S2; *, $p < 0.05$). This transgene-related behavioral phenotype has been noted in this and other mouse models of cerebral amyloidosis (10, 24-28), and may mirror disinhibition caused by cortical and/or hippocampal damage (29). Of interest, APP/PS1 transgene-associated hyperactivity, often taken as anxiety-like behavior in APP/PS1 mice, was completely reversed by combined treatment with EGCG plus FA (Fig. 1*B*, *left*; Table S2; †, $p < 0.05$, APP/PS1-EGCG/FA *versus* APP/PS1-EGCG or APP/PS1-FA mice). Combination treatment completely stabilized hyperactivity, as the co-treatment group did not significantly differ from any of the WT mouse groups (Fig. 1*B*, *left*; Table S2; $p > 0.05$).

Mice instinctively alternate arms in the Y-maze, such that they enter the three arms in sequence more often than by chance alone (50%, see dotted line in Fig. 1*B*, *right*; Table S2); this behavioral phenotype is generally interpreted as a measure of spatial working memory (24). As expected, APP/PS1-V mouse behavior revealed less tendency to alternate *versus* WT controls. One-way ANOVA followed by post hoc testing showed statistically significant differences on Y-maze spontaneous alternation between APP/PS1-V mice and the other seven mouse groups (Fig. 1*B*, *right*; Table S2; *, $p < 0.05$). Of note, EGCG- plus FA-treated APP/PS1 mice had greater % alternation compared with EGCG or FA single treatment (Fig. 1*B*, *right*; Table S2; ††, $p < 0.01$, APP/PS1-EGCG/FA *versus* APP/PS1-EGCG or APP/PS1-FA mice), which did not significantly differ from any of the WT mouse groups (Fig. 1*B*, *right*; Table S2; $p > 0.05$). Therefore, combination treatment fully restored defective spatial working memory in the alternation Y-maze.

Finally, we assessed hippocampus-dependent spatial reference learning and memory with the RAWM test. On day 1, overall ANOVA disclosed main effects of block ($p < 0.001$ for both errors and escape latency), genotype ($p < 0.05$ for errors and $p < 0.01$ for escape latency), and treatment ($p < 0.05$ for escape latency). APP/PS1-V mice tended toward increased number of errors and longer escape latencies to reach the visible or hidden platform locations compared with the other seven mouse groups. On day 2, overall ANOVA revealed main effects of block ($p < 0.001$ for both errors and escape latency), genotype ($p < 0.05$ for errors and $p < 0.01$ for escape latency), and treatment ($p < 0.001$ for both errors and escape latency). Repeated-measures ANOVA followed by post hoc assessment disclosed statistically significant differences between APP/PS1-V mice and the other seven mouse groups (Fig. 1, *C* and *D*, *left*; Tables S3 and S5; *, $p < 0.05$ for both errors and escape latency). APP/PS1-V mice had more errors and greater escape latencies to reach the visible or hidden platforms compared with the other seven mouse groups; yet, either singly- or doubly-treated APP/PS1 mice accomplished the task with significantly less errors and shorter latencies, and their behavior did not significantly differ from the four WT mouse groups (Fig. 1, *C* and *D*, *left* and *right*; Tables S3-S6; $p > 0.05$). There were no significant between-group differences ($p > 0.05$) on swim speed, nor did we find thigmotaxis (characteristic of extreme anxiety-like behavior) in any of the mice tested. Thus, behavioral differences in the RAWM test were not due to motivational issues, locomotor impairment, or anxiety. These results show that 3-month treatment with EGCG and/or FA completely remediates spatial reference learning and memory impairment associated with the *APP* and *PS1* transgenes. For all behavioral tests, sex was included as a categorical covariate in multiple ANOVA models, but we did not find significant main effects or interactive terms with sex ($p > 0.05$). Further, we stratified all



Downloaded from http://www.jbc.org/ by guest on January 9, 2019

analyses by sex and did not find any significant differences ($p > 0.05$; data not shown).

***Combination therapy mitigates cerebral amyloid pathology in APP/PS1 mice***

At 15 months of age, APP/PS1-V mice had progressive cerebral amyloid pathology (average of 7–8% cerebral β-amyloid burden) throughout retrosplenial cortex (RSC), entorhinal cortex (EC), and hippocampus (H) regions of interest (ROI). Treatment with EGCG (32–40%) or FA (29–35%) significantly reduced β-amyloid burden (by $A\beta_{17-24}$ monoclonal antibody 4G8) across all three brain regions (Figs. 2, *A-D* and 3, *A-C*; ***, $p \leq 0.001$). Importantly, combination therapy with EGCG plus FA further significantly mitigated cerebral amyloidosis in all three regions (50–60%) (Fig. 3, *A-C*; †, $p < 0.05$). To further examine if three-month treatment prevented *versus* reversed cerebral β-amyloid deposition, we included a separate cohort of eight untreated 12-month-old APP/PS1 mice (the age when dosing started) into the analysis (Fig. 3, *A-C*). Intriguingly, combined treatment trended toward reversing cerebral amyloid pathology across all three brain regions (Fig. 3, *A-C*). This effect was sex-independent (data not shown).

To determine if decreased cerebral β-amyloid burden was specific to a plaque subset or occurred more generally, we conducted morphometric analysis by blindly assigning β-amyloid plaques to one of three mutually exclusive categories according to maximum diameter: small (< 25 μm); medium (between 25 and 50 μm); or large (> 50 μm). Combination therapy with EGCG plus FA revealed significant reductions across all three plaque sizes: small (43–48%); medium (43–56%); and large (55–65%) (Figs. 2, *A-D* and 3, *D-F*; Tables S7-S9; *, $p < 0.05$; **, $p < 0.01$; ***, $p \leq 0.001$). Importantly, APP/PS1-EGCG/FA mice presented with additional reductions across all three plaque sizes and brain regions compared with either single treatment (Fig. 3, *D-F*; Tables S7-S9; †, $p < 0.05$; ††, $p < 0.01$); effects that were independent of sex (data not shown).

Like 83% of AD patients, APP/PS1 mice develop vascular β-amyloid deposits (cerebral amyloid angiopathy, CAA) with age (30), so we moved on to assess CAA pathology in our experimental paradigm. We blindly counted 4G8 antibody-stained cerebral vascular β-amyloid deposits in walls of penetrating arteries at the pial surface in RSC and EC areas, and in small arteries at the hippocampal fissure and brachium of the superior colliculus in the hippocampal region. Mean numbers of CAA deposits were significantly decreased in APP/PS1-EGCG (18–30%) and APP/PS1-FA (17–28%) mice, and were further reduced in APP/PS1-EGCG/FA mice (by 38–44%) *versus* APP/PS1-V mice in all three brain regions examined (Fig. 3*G*; Table S10; *, $p < 0.05$; **, $p < 0.01$; †, $p < 0.05$; ††, $p < 0.01$).

Importantly, we verified histological findings with biochemical analysis of Aβ species in brain homogenates using sandwich enzyme-linked immunosorbent assay (ELISA). In the TBS-soluble fraction, single- or double-treatment with EGCG/FA revealed significant reductions in $A\beta_{1-40}$ (30–59%) and $A\beta_{1-42}$ (38–53%) compared with APP/PS1-V mice (Fig. 4*A*; **, $p < 0.01$ for $A\beta_{1-40}$; *, $p < 0.05$ $A\beta_{1-42}$). $A\beta_{1-40}$ abundance was further reduced by combined treatment (Fig. 4*A*; †, $p < 0.05$). A similar trend was noted when considering the detergent-soluble fraction, where three single- or double-treatment APP/PS1 mouse groups significantly decreased in $A\beta_{1-40}$ (32–61%) and $A\beta_{1-42}$ (30–38%) (Fig. 4*B*; **, $p < 0.01$ for both $A\beta_{1-40}$ and $A\beta_{1-42}$) with additional reduction in $A\beta_{1-40}$ by combination therapy (Fig. 4*B*; †, $p < 0.05$). Lastly, the guanidine-HCl-soluble pellet, which most closely reflects β-amyloid deposits, disclosed marked reductions in APP/PS1-EGCG, -FA, or -EGCG/FA mouse groups for $A\beta_{1-40}$ (33–56%) and $A\beta_{1-42}$ (30–58%) (Fig. *4C*; ***, $p \leq 0.001$ for both $A\beta_{1-40}$ and $A\beta_{1-42}$). Here, combination therapy with EGCG plus FA demonstrated significant and additional reductions in both $A\beta_{1-40}$ and $A\beta_{1-42}$ abundance



Downloaded from http://www.jbc.org/ by guest on January 9, 2019

(Fig. *4C*; †, $p < 0.05$ for $A\beta_{1\text{-}40}$; ††, $p < 0.01$ for $A\beta_{1\text{-}42}$).

***Tandem modulation of APP cleavage by combination therapy***

Reduced cerebral amyloidosis in APP/PS1 mice after EGCG/FA treatment could be due to 1) increased brain-to-blood Aβ efflux (6), 2) reduced expression of *APP* or *PS1* transgenes, or 3) altered APP cleavage. We obtained peripheral blood samples from each APP/PS1 mouse group at the time of sacrifice and assayed plasma $A\beta_{1\text{-}40}$ and $A\beta_{1\text{-}42}$ species, but did not detect between-groups differences (data not shown). We then moved on to assess expression of transgene-derived APP or PS1 by Western blot in brain homogenates. Results showed comparable band densities; therefore, neither single nor dual treatment with EGCG/FA affected transgene-derived APP (Fig. 5*A*) or PS1 (data not shown) expression.

Having ruled out the first two possibilities, we moved on to elucidate if EGCG/FA therapy affected APP cleavage. We probed brain homogenates for APP metabolites as follows: nonamyloidogenic sAPP-α; amyloidogenic soluble APP-β, sAPP-β; β-carboxyl-terminal fragment, β-CTF/C99; phospho-β-CTF, P-β-CTF/P-C99; and monomeric/oligomeric Aβ species. While holo-APP was unchanged, densitometry confirmed that nonamyloidogenic APP cleavage to sAPP-α was significantly elevated in brain homogenates from both EGCG treatment groups (Fig. 5, *A* and *B*; Table S11; ***, $p < 0.001$ *versus* APP/PS1-V or APP/PS1-FA mice). Amyloidogenic APP cleavage to sAPP-β, C99, and P-C99 were significantly inhibited in brain homogenates in each treatment group (Fig. 5, *A*, *C*, and *D*; Table S11; ***, $p < 0.001$), and combination therapy further reduced sAPP-β as well as C99 and P-C99 band densities compared with either treatment alone (Fig. 5, *A*, *C*, and *D*; Table S11; ††, $p < 0.01$; †††, $p < 0.001$). Moreover, the 4-kDa monomeric Aβ band (Fig. 5*A*) and Aβ species between 25 and 75 kDa (putative Aβ oligomers, Fig. 5*A*) were also reduced in brain homogenates from three APP/PS1 mouse treatment groups. This was further supported by 82E1 sandwich ELISA for Aβ oligomers (Fig. 5*E*; **, $p < 0.01$ for APP/PS1-V *versus* treatment groups). It is noteworthy that combined treatment posted additional reductions across most measures of amyloidogenicity compared with EGCG or FA alone (Fig. 5*E*; ††, $p < 0.01$).

The above data provided evidence that combination therapy promoted nonamyloidogenic and inhibited amyloidogenic APP cleavage. To understand the molecular underpinnings of these findings, we examined ADAM10 (α-secretase candidate) and β-site APP cleaving enzyme 1 (BACE1, β-secretase) proteins by Western blot in brain homogenates from each group of APP/PS1 mice. As hypothesized, both precursor ADAM10 (pADAM10, 90-kDa band) and mature (active) ADAM10 (mADAM10, 68-kDa band) were elevated in brain homogenates from the two EGCG treatment groups, and densitometry confirmed significance (Fig. 6, *A-C*; Table S12; ***, $p < 0.001$ for pADAM10 and mADAM10). By contrast, BACE1 protein expression was lower in brain homogenates from treated *versus* APP/PS1-V mice, which we verified by densitometry (Fig. 6, *A* and *D*; Table S12; ***, $p < 0.001$). It is noteworthy that EGCG and FA co-treatment produced the greatest reduction in BACE1 expression (Fig. 6, *A* and *D*; Table S12; †††, $p < 0.001$). These results suggest that combination therapy elevates ADAM10 and decreases BACE1, thereby shifting toward nonamyloidogenic APP processing.

***Combination therapy alleviates neuroinflammation, oxidative stress, and synaptotoxicity in APP/PS1 mice***

In addition to anti-amyloidogenic properties, EGCG and FA have anti-inflammatory and anti-oxidant properties (10, 11, 13, 17, 18). Therefore, we moved on to investigate putative



Downloaded from http://www.jbc.org/ by guest on January 9, 2019

effects of each compound on neuroinflammatory processes and oxidative stress in APP/PS1 mice. We first examined β-amyloid deposit-associated gliosis (*i.e.* astrocytosis and microgliosis) by quantitative immunohistochemical analyses alongside brain mRNA expression of the cardinal proinflammatory innate immune cytokines, tumor necrosis factor-α (TNF-α) and interleukin-1β (IL-1β) by real-time polymerase chain reaction (QPCR). We also assayed brain mRNA expression of two key oxidative stress markers: superoxide dismutase 1 (SOD1) and glutathione peroxidase 1 (GPx1). APP/PS1-V mouse brains disclosed hyperplasia and hypertrophy of β-amyloid plaque-associated reactive astrocytes and microglia. We observed staining for the astrocytic activation marker, glial fibrillary acidic protein (GFAP), and the structural marker of activated microglia, ionized calcium-binding adapter molecule 1 (Iba1), in glial somata and processes. Numerous minute GFAP-positive astrocytic processes were distributed between neurons, and GFAP expression was intensely co-localized with dystrophic neurites associated with β-amyloid deposits (Fig. 7, *A-D*). All three mouse treatment groups had decreased reactive astrocytes and microglia, and quantitation revealed significant attenuation compared with APP/PS1-V mice (Fig. 8, *A-F*; ***, $p \leq 0.001$). Importantly, astrocytosis and microgliosis were further reduced in APP/PS1-EGCG/FA mice in all three brain regions examined (Fig. 8, *A-F*; †, $p < 0.05$; ††, $p < 0.01$). Supporting the above data, brain mRNA expression of TNF-α and IL-1β was significantly decreased in the three treatment groups compared with APP/PS1-V mice (Fig. 9*A*; Table S13; *, $p < 0.05$; **, $p < 0.01$). Combination therapy further significantly reduced brain proinflammatory cytokine expression compared with single treatments (Fig. 9*A*; Table S13; †, $p < 0.05$); brain expression of proinflammatory cytokines was completely blocked by co-treatment, and did not significantly differ from any of the WT control groups (Fig. 9*A*; Table S13; $p > 0.05$).

We noted a similar pattern of results for expression of key oxidative stress markers. APP/PS1-V brains had greater mRNA abundance of both SOD1 and GPx1 transcripts, and both were significantly reduced in the three treatment groups (Fig. 9*B*; Table S13; *, $p < 0.05$; **, $p < 0.01$). Combination therapy further significantly reduced brain expression of key oxidative stress markers compared with single treatment (Fig. 9*B*; Table S13; †, $p < 0.05$). Similar to proinflammatory cytokine mRNAs, combined treatment completely inhibited SOD1 and GPx1 mRNAs, which did not significantly differ from the three WT mouse groups (Fig. 9*B*; Table S13; $p > 0.05$). These effects were sex-independent (data not shown). Western blots on brain homogenates supported results presented above. In each treatment group, both SOD1 and GPx1 proteins were significantly reduced *versus* APP/PS1-V mice by densitometry (Fig. 9, *C-E*; Table S14; ***, $p < 0.001$). Strikingly, combination therapy showed further reduction compared with EGCG or FA treatment alone (Fig. 9, *C-E*; Table S14; †††, $p < 0.001$). Together, these results demonstrate that EGCG plus FA combination therapy stabilizes neuroinflammation and oxidative stress in APP/PS1 brains.

Finally, to evaluate whether combination therapy could ameliorate synaptotoxicity in APP/PS1 mice, we interrogated synaptophysin in hippocampal CA1 and EC regions. We noted elevated synaptophysin immunoreactivity (IR) in both brain areas from APP/PS1-EGCG, APP/PS1-FA, and APP/PS1-EGCG/FA mice compared with APP/PS1-V mice (Fig. 10, *A-F*; Table S15; ***, $p < 0.001$). Importantly, combination therapy produced strongest synaptophysin IR in both CA1 and EC regions that was further elevated *versus* either single treatment (Fig. 10, *A-F*; Table S15; †, $p < 0.05$).

## Discussion

A key drug development challenge is



Downloaded from http://www.jbc.org/ by guest on January 9, 2019

delivering an agent with few side effects that not only treats symptoms−but actually modifies disease. Here, we report that combination therapy with EGCG and FA completely reverses transgene-associated behavioral deficits in the APP/PS1 transgenic mouse model (see Fig. 1). In concert with learning and memory improvement, pathological findings demonstrate that combined therapy posts additional benefits over single treatments to attenuate parenchymal and vascular β-amyloidosis (see Figs. 2-4). In this regard, clinicopathological studies have investigated the relationship between cerebral amyloid pathology and cognitive deficits in human AD (31, 32). Similar to our results, numerous reports have linked reversal of transgene-associated behavioral deficits to attenuated cerebral amyloid pathology in mouse models (10, 26-28, 33-36), although others have shown that cognitive function and cerebral amyloidosis can be uncoupled (37, 38). In humans, elderly with preserved cognitive function reportedly have cerebral amyloid pathology comparable to prodromal or frank AD at autopsy (39, 40). One explanation provided for the discordancy between senile plaques and cognitive impairment in the human AD literature is that soluble, oligomeric forms of Aβ are the true neurotoxic species (41-44). In support of this hypothesis, others have demonstrated that behavioral deficit occurs in parallel with elevated Aβ oligomers in rodent models (34, 38). Interestingly, we show that combination treatment significantly decreases Aβ oligomers (see Fig. 5, which inversely correlates with cognitive function (see Fig. 1).

Sequential APP endoproteolysis by the secretases generates amyloidogenic C99 and sAPP-β followed by Aβ; whereas the nonamyloidogenic pathway generates sAPP-α and C83. Our data show significantly increased sAPP-α in brain homogenates from APP/PS1 mice treated with EGCG alone or in combination with FA; whereas sAPP-β, C99, and P-C99 production are reduced, providing evidence that APP cleavage is shifted toward the nonamyloidogenic pathway. Soluble APP-α has beneficial properties, including neurotrophism and neuroprotection (45, 46), and even enhancing long-term potentiation (47). Interestingly, treatment with EGCG alone not only increases nonamyloidogenic but also reduces amyloidogenic APP processing (see Fig. 5). Combined treatment significantly enhances protein expression of α-secretase candidate ADAM10, whereas BACE1 protein abundance is significantly reduced–even by EGCG treatment alone. This latter result is interesting, because a previous study showed that EGCG can act as a β-secretase modulator in a cell-free system (48). Nonetheless, combination therapy further significantly decreases BACE1 protein expression compared with EGCG alone (see Fig. 6). This agrees with our prior report that sAPP-α can indirectly modulate β-secretase activity and Aβ generation through a negative feedback loop (49), and others have shown that sAPP-α can autoregulate APP cleavage (50-52). Hence, EGCG can inhibit Aβ generation both by directly enhancing α-secretase and by indirectly modulating β-secretase activity. Collectively, our data show that combination therapy further polarizes APP cleavage towards nonamyloidogenic α-secretase cleavage *versus* either single treatment.

In the AD brain, reactive microglia and astrocytes co-exist in both temporal and spatial proximity to β-amyloid deposits, and glial activation leads to neuroinflammation that can cause bystander neuronal injury (53-55). Both EGCG and FA have additional beneficial properties, including reducing inflammation (10, 13, 18). Strikingly in fact, combination therapy confers greatest additional benefit over single treatments on neuroinflammation. When considering neuroinflammatory biomarkers, results show that combined treatment dampens plaque-associated microgliosis and astrocytosis and completely blocks brain mRNA expression of TNF-α and IL-1β to baseline levels (see Figs.



Downloaded from http://www.jbc.org/ by guest on January 9, 2019

7-9). Given the recent intense focus on inflammatory mechanisms in AD (54, 55), it remains possible that mitigated neuroinflammation after combination therapy plays a dominant role to reduce AD-like pathology and improve cognition in APP/PS1 mice.

Reactive oxygen species are produced during host defense against pathogens. However, when activated inappropriately or overproduced, oxidative substances can damage DNA, proteins and lipids, leading to cellular injury and death (56). Oxidative damage has been linked to AD pathogenesis (57, 58), and both EGCG and FA have anti-oxidant and free radical scavenging properties (10, 11, 13, 17). Therefore, we explored whether the compounds modulated oxidative stress in APP/PS1 mice. Results show that combined treatment with EGCG and FA completely reduces cerebral mRNA expression of SOD1 and GPx1 to baseline levels in APP/PS1 mice, while EGCG or FA single treatment has only modest effects. We actually observe greatest reductions in SOD1 or GPx1 proteins with combination therapy (see Fig. 9).

Synaptic loss is a cardinal feature of the AD brain, and the role of Aβ in synapse loss and dysfunction is well-documented. Importantly, synaptic plasticity is considered to form the cellular basis for learning and memory (59-61). Dysregulated plasticity leads to synaptic loss, and decreased synapse distribution is a durable predictor of disease progression and behavioral decline (59). Synaptophysin is a pre-synaptic marker that is mostly commonly used as a surrogate for synaptic density (62). In this regard, we quantified synaptophysin IR in hippocampal CA1 and EC regions of APP/PS1 mice and found significant increases in each APP/PS1 treatment group, with greatest benefit after combined treatment (see Fig. 10).

Even more than with single treatment approaches, safety is a key issue with combination therapy, and adverse effects must be taken into account. Importantly, single or dual treatment with EGCG and FA for 3 months is well-tolerated−we did not observe any adverse events in any of the mice included in our study. Based on the chemical database for EGCG by Registry of Toxic Effects of Chemical Substances, acute oral lethal dose for 50% ($LD_{50}$) is as high as 2,710 mg/kg in mice. Likewise, FA has a high acute oral $LD_{50}$ of 2,370 mg/kg in mice (10), with a human equivalent dose of 2.43 mg/kg for EGCG or FA, which equates to a 146 mg dose for a 60 kg person (63). Moreover, the tolerable daily intake in a human can be extrapolated from rodent $LD_{50}$ threshold data (64). Assuming the body surface area calculation factor for interspecies variation (63), the tolerable human daily intake for EGCG is equivalent to 13.18 g, whereas FA is 11.53 g (both assume 60 kg human weight). Thus, the doses (30 mg/kg/day for a mouse: 146 mg for a human) used in this study are quite low, and such advantageous pharmacotoxicity profiles reinforce the notion that combined EGCG/FA administration is safe. Nonetheless, it remains possible that increased ADAM10 and/or decreased BACE1 activity might also affect processing of other substrates, leading to unwanted side effects. Hence, further translational research is warranted to investigate whether long-term EGCG and FA therapy is safe in humans.

With respect to the pharmacokinetics of EGCG in humans, the compound is absorbed at < 5% abundance and reaches peak plasma concentration time ($T_{max}$) at 2 h after per os administration (65, 66). Green tea catechins are primarily absorbed in the intestine (*i.e.* jejunum and ileum) by paracellular diffusion through epithelial cells (67). Once absorbed, free EGCG is mainly detected in plasma (> 75%) (14, 68) and has a half-life (T1/2) of ~3 h (65, 66). Similar to EGCG, FA is absorbed from the stomach, jejunum, and ileum. Free FA can be found in human plasma just 10 min after oral administration of sodium ferulate (69). Plasma FA concentrations reach $T_{max}$ at 24 min following oral administration, with a T1/2 of 42 min (69).



Downloaded from http://www.jbc.org/ by guest on January 9, 2019

Free FA and its glucuronic conjugate are detected in the plasma, and both free FA and its glycine conjugate are found in urine after ingestion of FA containing wheat bran (70). The urinary excretion of FA in humans plateaus between 7 h and 9 h after ingestion (71).

An important question is whether EGCG and FA can cross the blood-brain barrier. Using liquid chromatography coupled with tandem mass spectrometry electrospray ionization, EGCG was detected in the rodent brain after systemic administration (16). With respect to FA, standard high-performance liquid chromatography approaches have detected the compound in the brain after peripheral administration (22, 23). This result has been validated using a more advanced technique; ultra-performance liquid chromatography coupled to tandem mass spectrometry (72).

The vast majority (> 95%) of AD cases are 'sporadic'; characterized by onset at 65 years or later, while less than 5% of cases are early-onset autosomal dominant AD. To date, a series of mutations in three different genes (*i.e., APP*, *PS1*, and *PS2*) cause autosomal dominant AD (73). These mutations have been used to varying degrees to study basic and translational aspects of AD. One of the most widely used tools is transgenic mice expressing one or more of these mutant human transgenes. In this study, we utilized APP/PS1 mice harboring human *APP* and *PS1* mutations. It is important to note that, while APP/PS1 mice model some of the AD relevant phenotypes including cerebral amyloidosis, neuroinflammation, and cognitive disturbance, they do not recapitulate all AD features and are therefore not a complete model of human AD.

In conclusion, we report that administering 3-month combination therapy with EGCG and FA to the aged APP/PS1 transgenic mouse model of cerebral amyloidosis confers additional benefits over single treatments on improving behavioral deficits, ameliorating cerebral amyloidosis, and reducing Aβ generation. Further, combined treatment potently stabilizes neuroinflammation, alleviates oxidative stress, and mitigates synaptotoxicity. We propose long-term combination therapy with EGCG and FA as an effective disease-modifying therapy for AD.

## Experimental procedures

### *Ethics statement*

All experiments were performed in accordance with the guidelines of the National Institutes of Health, and all animal studies were approved by the Saitama Medical University Institutional Animal Care and Use Committee. Animals were humanely cared for during all experiments, and all efforts were made to minimize suffering.

### *Mice*

Male B6.Cg-Tg($APP_{swe}$, PSEN1dE9)85Dbo/Mmjax mice (bearing "Swedish" $APP_{K595N/M596L}$ and *PS1* exon 9-deleted mutant human transgenes) on the congenic C57BL/6J background (designated APP/PS1 mice) (74) and female C57BL/6J mice were obtained from The Jackson Laboratory (Bar Harbor, ME). For colony maintenance, male APP/PS1 mice on the congenic C57BL/6J background were bred with female C57BL/6J mice to yield APP/PS1 and WT offspring–so all experimental APP/PS1 mice and WT littermates in this study are on the same C57BL/6J genetic background.

EGCG and FA were obtained from Sigma-Aldrich (St. Louis, MO). Twenty mg of each reagent was resuspended in 25 µl of 100% dimethyl sulfoxide and then diluted with distilled water to a final concentration of 0.2% dimethyl sulfoxide. All regents were freshly prepared daily prior to each treatment. We randomly assigned APP/PS1 mice to four treatment groups ($n$ = 8 per condition; four males and four females): EGCG (APP/PS1-EGCG); FA (APP/PS1-FA); EGCG + FA (APP/PS1-EGCG/FA); or vehicle (distilled water containing dimethyl sulfoxide at a final concentration of



Downloaded from http://www.jbc.org/ by guest on January 9, 2019

0.2%; APP/PS1-V). Additionally, WT littermates received the same four treatments (*n* = 8 per group; four males and four females) as follows: WT-EGCG; WT-FA; WT-EGCG/FA mice; or vehicle (WT-V). To determine whether treatment prevented *versus* reversed kinetics of cerebral amyloid accumulation, we included eight untreated APP/PS1 mice at 12 months of age (APP/PS1-12M mice, four males and four females) for analysis of β-amyloid pathology. After baseline behavioral assessment just before dosing (12 months of age), animals were gavaged with EGCG, FA, EGCG plus FA (all at 30 mg/kg), or vehicle once daily for 3 months. Mice were housed in a specific pathogen-free barrier facility under a 12/12-h light/dark cycle with *ad libitum* access to food and water.

***Behavioral analyses***

To assess novel object recognition and retention, animals were habituated in a cage for 4 h, and two objects of different shapes were concurrently provided for 10 min. The number of times that the animal explored the familiar object (defined as number of instances where an animal directed its nose 2 cm or less from the object) was counted for the initial 5 min of exposure (training phase). To test memory retention on the following day, one of the familiar objects was replaced with a different shaped novel object and explorations were recorded for 5 min (retention test). The recognition index, taken as a measurement of episodic memory, is reported as frequency (%) of explorations of the novel *versus* familiar objects (75).

To measure exploratory activity and spatial working memory, animals were individually placed in one arm of a radially symmetric Y-maze made of opaque gray acrylic (arms, 40 cm long and 4 cm wide; walls, 30 cm tall), and the sequence of arm entries and total number of entries were counted over a period of 8 min, beginning when the animal first entered the central area. Percent alternation was defined as entries into sequentially different arms on consecutive occasions using the following formula: % alternation = number of alternations/(number of total arm entries − 2) × 100% (24).

To assess spatial reference learning and memory, the RAWM test was conducted over 2 days and consisted of triangular wedges in a circular pool (80 cm diameter) configured to form swim lanes that enclose a central open space. Mice naïve to the task were placed in the pool and allowed to search for the platform for 60 s. Animals were dropped into a random start arm and allowed to swim until they located and climbed onto the platform (goal) over a period of 60 s. Latency to locate the platform and errors were recorded. Each mouse was given a total of 15 trials. On day 1, the goal alternated between visible and hidden; although on day 2, the goal was always hidden. All data were organized as individual blocks of three trials each. The goal arms remained in the same location for both days, whereas the start arm was randomly altered. All trials were done at the same time of day (± 1 h), during the animals' light phase. To avoid interference with behavioral testing, each treatment was carried out 1 h after concluding behavioral testing (76).

***Brain tissue preparation***

At 15 months of age, animals were anesthetized with sodium pentobarbital (50 mg/kg) and euthanized by transcardial perfusion with ice-cold physiological saline containing heparin (10 units/ml). Brains were isolated and quartered (sagittally at the level of the longitudinal fissure of the cerebrum, and then coronally at the level of the anterior commissure). Left anterior hemispheres were weighed and snap-frozen at -80°C for Western blot analysis. Right anterior hemispheres were weighed and immersed in RNA stabilization solution (RNAlater®, Applied Biosystems, Foster City, CA) and then snap-frozen at -80°C for QPCR analysis. Left posterior hemispheres were



Downloaded from http://www.jbc.org/ by guest on January 9, 2019

immersed in 4% paraformaldehyde at 4°C overnight and routinely processed in paraffin. Right posterior hemispheres were weighed and snap-frozen at -80°C for ELISA.

***Immunohistochemistry***

Five coronal paraffin sections (per set) were cut with a 100-μm interval and 5-μm thickness spanning bregma –2.92 to –3.64 mm (77). Three sets of five sections were prepared for analyses of Aβ deposits/β-amyloid plaques, astrocytosis, and microgliosis. An additional set of five sections was used for analysis of synaptophysin IR. Primary antibodies were as follows: biotinylated anti-$A\beta_{17-24}$ monoclonal (1:200 dilution, 4G8; Covance Research Products, Emeryville, CA); anti-GFAP polyclonal (1:500 dilution, Dako, Carpinteria, CA); carboxyl-terminal anti-Iba1 polyclonal (1:500 dilution, FUJIFILM Wako Pure Chemical, Osaka, Japan); and carboxyl-terminal anti-synaptophysin monoclonal (1:20 dilution, DAK-SYNAP; Dako) antibodies. Immunohistochemistry was performed using a Vectastain ABC *Elite* Kit (Vector Laboratories, Burlingame, CA) coupled with the diaminobenzidine reaction, except that the biotinylated secondary antibody step was omitted for the biotinylated $A\beta_{17-24}$ monoclonal antibody.

***Image analysis***

Images were acquired and quantified using SimplePCI software (Hamamatsu Photonics, Shizuoka, Japan). Images of five 5-μm sections through each anatomic ROI (*i.e.* RSC, EC, and H) were captured based on anatomical criteria (77), and we set a threshold optical density that discriminated staining from background. Selection bias was controlled for by analyzing each ROI in its entirety. For Aβ, GFAP, and Iba1 burden analyses, data are reported as the percentage of positive pixels captured divided by the full area captured. For conventional Aβ burden analysis, the $A\beta_{17-24}$ monoclonal antibody was used; its epitope that lies within amino acids 18-22 (VFFAE).

For β-amyloid plaque morphometric analysis, diameters (maximum lengths) of β-amyloid plaques were measured, and three mutually exclusive plaque size categories (< 25, 25–50, or > 50 μm) were blindly tabulated. For quantitative analysis of CAA, numbers of Aβ antibody-positive cerebral vessels were blindly counted in each ROI. To evaluate synaptophysin IR, images of five 5-μm sections through hippocampal CA1 and EC were blindly captured based on anatomical criteria (77) and converted to gray scale. The average optical density of positive signals from each image was quantified as a relative number from zero (white) to 255 (black) and expressed as mean intensity of synaptophysin IR.

***ELISA***

Brain $A\beta_{1-40}$ and $A\beta_{1-42}$ species were detected by a three-step extraction protocol with modifications (78). Brains were homogenized using TissueLyser LT (Qiagen, Valencia, CA) in Tris-buffered saline (TBS: 25 mM Tris-HCl, pH 7.4, 150 mM NaCl) containing protease inhibitor cocktail (Sigma-Aldrich) and centrifuged at 18,800 × *g* for 60 min at 4°C, and supernatants were collected (representing the TBS-soluble fraction). Resulting pellets were treated with TNE buffer (10 mM Tris-HCl, 1% Nonidet P-40, 1 mM EDTA, and 150 mM NaCl) with protease inhibitors and homogenized using TissueLyser LT. Homogenates were then centrifuged at 18,800 × *g* for 30 min at 4°C, and supernatants were collected (representing the detergent-soluble fraction). Remaining pellets were treated with 5 M guanidine HCl and dissolved by occasional mixing on ice for 30 min and centrifuged at 18,800 × *g* for 30 min at 4°C. Supernatants were then collected; this is taken as the guanidine HCl-soluble fraction. $A\beta_{1-40}$ and $A\beta_{1-42}$ species were separately quantified in each sample in duplicate by sandwich ELISA (IBL, Gunma, Japan) (79). Aβ oligomers were quantified in the TNE-soluble fraction in



Downloaded from http://www.jbc.org/ by guest on January 9, 2019

duplicate by Human Amyloidβ Oligomers (82E1-specific) Assay Kit (IBL) (80). All samples fell within the linear range of the standard curve.

***Western blot***

Brain homogenates were lysed in TBS containing protease inhibitor cocktail (Sigma-Aldrich) followed by TNE buffer, and aliquots corresponding to 10 μg of total protein (equally loaded per lane) were electrophoretically separated for each mouse brain using Tris glycine gels. Electrophoresed proteins were transferred to polyvinylidene difluoride membranes (Bio-Rad, Richmond, CA) that were blocked for 1 h at ambient temperature. Membranes were then hybridized for 1 h at ambient temperature with primary antibodies to follows: amino-terminal anti-APP polyclonal (1:2,000 dilution, IBL); carboxyl-terminal anti-presenilin 1 (PS1) monoclonal (1:500 dilution, PS1-loop, Merck Millipore, Darmstadt, Germany); carboxyl-terminal anti-sAPP-α monoclonal (1:300 dilution, 2B3; IBL); carboxyl-terminal anti-sAPPβ-sw monoclonal (1:100 dilution, 6A1; IBL), amino-terminal anti-$Aβ_{1-16}$ monoclonal (1:500 dilution, 82E1; IBL); carboxyl-terminal anti-BACE1 polyclonal (1:400 dilution, IBL); carboxyl-terminal anti-ADAM10 polyclonal (1:1,500 dilution, Cell Signaling Technology, Danvers, MA); anti-Cu/Zn SOD polyclonal (1:3,000 dilution, Enzo Life Sciences, Farmingdale, NY); anti-GPx1 polyclonal (1:4,000 dilution, Boster Biological Technology, Pleasanton, CA); and anti-β-actin monoclonal (1:5,000 dilution, 13E5; Cell Signaling Technology; as a loading control). Membranes were then rinsed and incubated for 1 h at ambient temperature with appropriate horseradish peroxidase-conjugated secondary antibodies (1:50,000 dilution for both primary monoclonal and polyclonal antibodies). After additional rinsing, membranes were incubated for 5 min at ambient temperature with enhanced chemiluminescence substrate (SuperSignal West Dura Extended Duration Substrate, Thermo Fisher Scientific, Waltham, MA), exposed to film, and developed. Western blots were done for each brain (n = 8 mice per group) and quantitative data were averaged.

***QPCR***

We quantified TNF-α, IL-1β, SOD1, GPx1, and β-actin mRNA levels by QPCR analyses (10, 26, 27). Total RNA was extracted using the RNeasy Mini Kit (Qiagen), and first strand cDNA synthesis was carried out using the QuantiTect Reverse Transcription Kit (Qiagen) in accordance with the manufacturer's instructions. We diluted cDNA 1:1 in $H_2O$ and carried out QPCR for all genes of interest using cDNA-specific TaqMan primer/probe sets (TaqMan Gene Expression Assays, Applied Biosystems) on an ABI 7500 Fast Real-time PCR instrument (Applied Biosystems). Each 20-μL reaction mixture contained 2 μl of cDNA with 1 μl of TaqMan Gene Expression Assay reagent, 10 μl of TaqMan Fast Universal PCR Master Mix (Applied Biosystems), and 7 μl of $H_2O$. Thermocycler conditions consisted of: 95°C for 15 s, followed by 40 cycles of 95°C for 1 s and 60°C for 20 s. Mouse TaqMan probe/primer sets were as follows: TNF-α (number Mm00443258_m1); IL-1β (number Mm00434228_m1); SOD1 (number Mm01700393_g1); GPx1 (number Mm00656767_g1); and β-actin (number Mm00607939_s1; used as an internal reference control) (Applied Biosystems). Samples that were not subjected to reverse transcription were run in parallel as negative controls to rule out genomic DNA contamination, and a "no template control" was also included for each primer set. The cycle threshold number ($C_T$) method (81) was used to determine relative amounts of initial target cDNA in each sample. Results are expressed relative to vehicle control WT mice.

***Statistical analysis***

Data are presented as means with associated standard deviations. A hierarchical analysis



Downloaded from http://www.jbc.org/ by guest on January 9, 2019

strategy was used in which the first step was an overall ANOVA (repeated measures was used for behavioral data) to assess significance of main effects and interactive terms. If significant, post hoc testing was done with Tukey's HSD or Dunnett's T3 methods, where appropriateness was determined based on Levene's test for equality of the variance. In instances of multiple mean comparisons, one-way ANOVA was used, followed by post hoc comparison of the means using Bonferroni's or Dunnett's T3 methods (depending on Levene's test for equality of the variance). The α levels were set at 0.05 for all analyses. All analyses were performed using the Statistical Package for the Social Sciences, release 23.0 (IBM SPSS, Armonk, NY).

**ACKNOWLEDGEMENTS** This work was supported, in whole or in part, by National Institutes of Health Grants 2R01NS076794-06A1, 1RF1AG053982-01A1, 5P01AG052350-03 and 5R21AG053884-02 (to T. T.), the Japan Society for the Promotion of Science KAKENHI JP26430058 (to T. M.), an Alzheimer's Association Sex and Gender in Alzheimer's disease grant (SAGA; to T. T.), Cure Alzheimer's Fund (to T. T.), Coins for Alzheimer's Research Trust (to T. T.), and generous start-up funds from the Zilkha Neurogenetic Institute of the Keck School of Medicine at the University of Southern California (to T. T.).

**CONFLICT OF INTEREST**

The authors declare that they have no conflicts of interest with the contents of this article. The content is solely the responsibility of the authors and does not necessarily represent the official views of the National Institutes of Health.

**AUTHOR CONTRIBUTIONS**

T.M. and T.T. designed the study, analyzed the data, and wrote the paper. T.M., N.K., T.S., J.T., and M.M. performed the experiments. All authors reviewed the results and approved the final version of the manuscript.

Downloaded from http://www.jbc.org/ by guest on January 9, 2019

**REFERERENCES**


1. Selkoe, D. J. (2001) Alzheimer's disease: genes, proteins, and therapy. *Physiol. Rev.* **81**, 741-766
2. De Strooper, B., Saftig, P., Craessaerts, K., Vanderstichele, H., Guhde, G., Annaert, W., Von Figura, K., and Van Leuven, F. (1998) Deficiency of presenilin-1 inhibits the normal cleavage of amyloid precursor protein. *Nature* **391**, 387-390
3. Sinha, S., and Lieberburg, I. (1999) Cellular mechanisms of β-amyloid production and secretion. *Proc. Natl. Acad. Sci. U.S.A.* **96**, 11049-11053
4. Vassar, R., Bennett, B. D., Babu-Khan, S., Kahn, S., Mendiaz, E. A., Denis, P., Teplow, D. B., Ross, S., Amarante, P., Loeloff, R., Luo, Y., Fisher, S., Fuller, J., Edenson, S., Lile, J., *et al.* (1999) β-secretase cleavage of Alzheimer's amyloid precursor protein by the transmembrane aspartic protease BACE. *Science* **286**, 735-741
5. Kimberly, W. T., LaVoie, M. J., Ostaszewski, B. L., Ye, W., Wolfe, M. S., and Selkoe, D. J. (2003) γ-secretase is a membrane protein complex comprised of presenilin, nicastrin, Aph-1, and Pen-2. *Proc. Natl. Acad. Sci. U.S.A.* **100**, 6382-6387
6. DeMattos, R. B., Bales, K. R., Cummins, D. J., Paul, S. M., and Holtzman, D. M. (2002) Brain to plasma amyloid-β efflux: a measure of brain amyloid burden in a mouse model of Alzheimer's disease. *Science* **295**, 2264-2267
7. Postina, R., Schroeder, A., Dewachter, I., Bohl, J., Schmitt, U., Kojro, E., Prinzen, C., Endres, K., Hiemke, C., Blessing, M., Flamez, P., Dequenne, A., Godaux, E., van Leuven, F., and Fahrenholz, F. (2004) A disintegrin-metalloproteinase prevents amyloid plaque formation and hippocampal defects in an Alzheimer disease mouse model. *J. Clin. Invest.* **113**, 1456-1464
8. Rezai-Zadeh, K., Shytle, D., Sun, N., Mori, T., Hou, H., Jeanniton, D., Ehrhart, J., Townsend, K., Zeng, J., Morgan, D., Hardy, J., Town, T., and Tan, J. (2005) Green tea epigallocatechin-3-gallate (EGCG) modulates amyloid precursor protein cleavage and reduces cerebral amyloidosis in Alzheimer transgenic mice. *J. Neurosci.* **25**, 8807-8814
9. Obregon, D.F., Rezai-Zadeh, K., Bai, Y., Sun, N., Hou, H., Ehrhart, J., Zeng, J., Mori, T., Arendash, G.W., Shytle, D., Town, T., and Tan, J. (2006) ADAM10 activation is required for green tea (−)-epigallocatechin-3-gallate-induced α-secretase cleavage of amyloid precursor protein. *J. Biol. Chem.* **281**, 16419-16427
10. Mori, T., Koyama, N., Guillot-Sestier, M. V., Tan, J., and Town, T. (2013) Ferulic acid is a nutraceutical β-secretase modulator that improves behavioral impairment and Alzheimer-like pathology in transgenic mice. *PLoS ONE* **8**, e55774
11. Legeay, S., Rodier, M., Fillon, L., Faure, S., and Clere, N. (2015) Epigallocatechin Gallate: A Review of Its Beneficial Properties to Prevent Metabolic Syndrome. *Nutrients* **7**, 5443-5468
12. Bhagwat, S., Haytowitz, D.B., Holden, and J.M. (2011) *USDA Database for the Flavonoid Content of Selected Foods. Release 3.* Nutrient Data Laboratory, Beltsville Human Nutrition Research Center, Agricultural Research Service, U.S. Department of Agriculture. http://www.ars.usda.gov/nutrientdata
13. Singh, N.A., Mandal, A.K., Khan, and Z.A. (2016) Potential neuroprotective properties of epigallocatechin-3-gallate (EGCG). *Nutr. J.* **15**, 60
14. Lee, M.J., Maliakal, P., Chen, L., Meng, X., Bondoc, F.Y., Prabhu, S., Lambert, G., Mohr, S., and Yang, C.S. (2002) Pharmacokinetics of tea catechins after ingestion of green tea and (−)-epigallocatechin-3-gallate by humans: formation of different metabolites and individual variability. *Cancer Epidemiol. Biomarkers Prev.* **11**, 1025-1032




Downloaded from http://www.jbc.org/ by guest on January 9, 2019

15. van't Slot, G., and Humpf, H.U. (2009) Degradation and metabolism of catechin, epigallocatechin-3-gallate (EGCG), and related compounds by the intestinal microbiota in the pig cecum model. *J. Agric. Food Chem.* **57**, 8041-8048
16. Lin, L.C., Wang, M.N., Tseng, T.Y., Sung, J.S., and Tsai, T.H. (2007) Pharmacokinetics of (−)-epigallocatechin-3-gallate in conscious and freely moving rats and its brain regional distribution. *J. Agric. Food Chem.* **55**, 1517-1524
17. Kanski, J., Aksenova, M., Stoyanova, A., and Butterfield, D. A. (2002) Ferulic acid antioxidant protection against hydroxyl and peroxyl radical oxidation in synaptosomal and neuronal cell culture systems in vitro: structure-activity studies. *J. Nutr. Biochem.* **13**, 273-281
18. Srinivasan, M., Sudheer, A.R., and Menon, V.P. (2007) Ferulic acid: therapeutic potential through its antioxidant property. *J. Clin. Biochem. Nutr.* **40**, 92-100
19. Zhao, Z., Egashira, Y., and Sanada, H. (2004) Ferulic acid is quickly absorbed from rat stomach as the free form and then conjugated mainly in liver. *J. Nutr.* **134**, 3083-3088
20. Zhao, Z., and Moghadasian, M. H. (2008) Chemistry, natural sources, dietary intake and pharmacokinetic properties of ferulic acid: a review. *Food Chem.* **109**, 691-702
21. Sultana, R., Ravagna, A., Mohmmad-Abdul, H., Calabrese, V., and Butterfield, D. A. (2005) Ferulic acid ethyl ester protects neurons against amyloid β-peptide(1-42)-induced oxidative stress and neurotoxicity: relationship to antioxidant activity. *J. Neurochem.* **92**, 749-758
22. Qin, J., Chen, D., Lu, W., Xu, H., Yan, C., Hu, H., Chen, B., Qiao, M., and Zhao, X. (2008) Preparation, characterization, and evaluation of liposomal ferulic acid *in vitro* and *in vivo*. *Drug Dev. Ind. Pharm.* **34**, 602-608
23. Wu, K., Wang, Z.Z., Liu, D., and Qi, X.R. (2014) Pharmacokinetics, brain distribution, release and blood-brain barrier transport of *Shunaoxin* pills. *J. Ethnopharmacol.* **151**, 1133-1140
24. Arendash, G. W., King, D. L., Gordon, M. N., Morgan, D., Hatcher, J. M., Hope, C. E., and Diamond, D. M. (2001) Progressive, age-related behavioral impairments in transgenic mice carrying both mutant amyloid precursor protein and presenilin-1 transgenes. *Brain Res.* **891**, 42-53
25. King, D. L., Arendash, G. W., Crawford, F., Sterk, T., Menendez, J., and Mullan, M. J. (1999) Progressive and gender-dependent cognitive impairment in the $APP_{SW}$ transgenic mouse model for Alzheimer's disease. *Behav. Brain Res.* **103**, 145-162
26. Town, T., Laouar, Y., Pittenger, C., Mori, T., Szekely, C. A., Tan, J., Duman, R. S., and Flavell, R. A. (2008) Blocking TGF-β-Smad2/3 innate immune signaling mitigates Alzheimer-like pathology. *Nat. Med.* **14**, 681-687
27. Mori, T., Rezai-Zadeh, K., Koyama, N., Arendash, G. W., Yamaguchi, H., Kakuda, N., Horikoshi-Sakuraba, Y., Tan, J., and Town, T. (2012) Tannic acid is a natural β-secretase inhibitor that prevents cognitive impairment and mitigates Alzheimer-like pathology in transgenic mice. *J. Biol. Chem.* **287**, 6912-6927
28. Mori, T., Koyama, N., Segawa, T., Maeda, M., Maruyama, N., Kinoshita, N., Hou, H., Tan, J., and Town, T. (2014) Methylene blue modulates β-secretase, reverses cerebral amyloidosis, and improves cognition in transgenic mice. *J. Biol. Chem.* **289**, 30303-30317
29. Kim, K. S., and Han, P. L. (2006) Optimization of chronic stress paradigms using anxiety- and depression-like behavioral parameters. *J. Neurosci. Res.* **83**, 497-507
30. Ellis, R.J., Olichney, J.M., Thal, L.J., Mirra, S.S., Morris, J.C., Beekly, D., and Heyman, A. (1996) Cerebral amyloid angiopathy in the brains of patients with Alzheimer's disease: the CERAD experience, Part XV. *Neurology* **46**, 1592-1596



Downloaded from http://www.jbc.org/ by guest on January 9, 2019

31. Sabbagh, M.N., Cooper, K., DeLange, J., Stoehr, J.D., Thind, K., Lahti, T., Reisberg, B., Sue, L., Vedders, L., Fleming, S.R., and Beach, T.G. (2010) Functional, global and cognitive decline correlates to accumulation of Alzheimer's pathology in MCI and AD. *Curr. Alzheimer Res.* **7**, 280-286
32. Robinson, J.L., Geser, F., Corrada, M.M., Berlau, D.J., Arnold, S.E., Lee, V.M., Kawas, C.H., and Trojanowski, J.Q. (2011) Neocortical and hippocampal amyloid-β and tau measures associate with dementia in the oldest-old. *Brain* **134**, 3708-3715
33. Schenk, D., Barbour, R., Dunn, W., Gordon, G., Grajeda, H., Guido, T., Hu, K., Huang, J., Johnson-Wood, K., Khan, K., Kholodenko, D., Lee, M., Liao, Z., Lieberburg, I., Motter, R., *et al.* (1999) Immunization with amyloid-β attenuates Alzheimer-disease-like pathology in the PDAPP mouse. *Nature* **400**, 173-177
34. Kotilinek, L. A., Bacskai, B., Westerman, M., Kawarabayashi, T., Younkin, L., Hyman, B. T., Younkin, S., and Ashe, K. H. (2002) Reversible memory loss in a mouse transgenic model of Alzheimer's disease. *J. Neurosci.* **22**, 6331-6335
35. Hartman, R. E., Izumi, Y., Bales, K. R., Paul, S. M., Wozniak, D. F., and Holtzman, D. M. (2005) Treatment with an amyloid-β antibody ameliorates plaque load, learning deficits, and hippocampal long-term potentiation in a mouse model of Alzheimer's disease. *J. Neurosci.* **25**, 6213-6220
36. Mouri, A., Noda, Y., Hara, H., Mizoguchi, H., Tabira, T., and Nabeshima, T. (2007) Oral vaccination with a viral vector containing Aβ cDNA attenuates age-related Aβ accumulation and memory deficits without causing inflammation in a mouse Alzheimer model. *FASEB J.* **21**, 2135-2148
37. Holcomb, L. A., Gordon, M. N., Jantzen, P., Hsiao, K., Duff, K., and Morgan, D. (1999) Behavioral changes in transgenic mice expressing both amyloid precursor protein and presenilin-1 mutations: lack of association with amyloid deposits. *Behav. Genet.* **29**, 177-185
38. Westerman, M. A., Cooper-Blacketer, D., Mariash, A., Kotilinek, L., Kawarabayashi, T., Younkin, L. H., Carlson, G. A., Younkin, S. G., and Ashe, K. H. (2002) The relationship between Aβ and memory in the Tg2576 mouse model of Alzheimer's disease. *J. Neurosci.* **22**, 1858-1867
39. Price, J.L., McKeel, D.W. Jr., Buckles, V.D., Roe, C.M., Xiong, C., Grundman, M., Hansen, L.A., Petersen, R.C., Parisi, J.E., Dickson, D.W., Smith, C.D., Davis, D.G., Schmitt, F.A., Markesbery, W.R., Kaye, J. , *et al.* (2009) Neuropathology of nondemented aging: Presumptive evidence for preclinical Alzheimer disease. *Neurobiol. Aging* **30**, 1026-1036
40. Mufson, E.J., Malek-Ahmadi, M., Perez, S.E., and Chen, K. (2016) Braak staging, plaque pathology, and APOE status in elderly persons without cognitive impairment. *Neurobiol. Aging* **37**, 147-153
41. Walsh, D. M., Klyubin, I., Fadeeva, J. V., Cullen, W. K., Anwyl, R., Wolfe, M. S., Rowan, M. J., and Selkoe, D. J. (2002) Naturally secreted oligomers of amyloid β protein potently inhibit hippocampal long-term potentiation *in vivo*. *Nature* **416**, 535-539
42. Cleary, J. P., Walsh, D. M., Hofmeister, J. J., Shankar, G. M., Kuskowski, M. A., Selkoe, D. J., and Ashe, K. H. (2005) Natural oligomers of the amyloid-β protein specifically disrupt cognitive function. *Nat. Neurosci.* **8**, 79-84
43. Haass, C., and Selkoe, D.J. (2007) Soluble protein oligomers in neurodegeneration: lessons from the Alzheimer's amyloid β-peptide. *Nat. Rev. Mol. Cell Biol.* **8**, 101-112
44. Shankar, G. M., Li, S., Mehta, T. H., Garcia-Munoz, A., Shepardson, N. E., Smith, I., Brett, F. M., Farrell, M. A., Rowan, M. J., Lemere, C. A., Regan, C. M., Walsh, D. M., Sabatini, B. L.,



Downloaded from http://www.jbc.org/ by guest on January 9, 2019

and Selkoe, D. J. (2008) Amyloid-β protein dimers isolated directly from Alzheimer's brains impair synaptic plasticity and memory. *Nat. Med.* **14**, 837-842

45. Mattson, M. P., Cheng, B., Culwell, A. R., Esch, F.S., Lieberburg, I., and Rydel, R. E. (1993) Evidence for excitoprotective and intraneuronal calcium-regulating roles for secreted forms of the β-amyloid precursor protein. *Neuron* **10**, 243-254
46. Mattson, M. P. (1997) Cellular actions of β-amyloid precursor protein and its soluble and fibrillogenic derivatives. *Physiol. Rev.* **77**, 1081-1132
47. Ishida, A., Furukawa, K., Keller, J. N., and Mattson, M. P. (1997) Secreted form of β-amyloid precursor protein shifts the frequency dependency for induction of LTD, and enhances LTP in hippocampal slices. *Neuroreport* **8**, 2133-2137
48. Jeon, S.Y., Bae, K., Seong, Y.H., and Song, K.S. (2003) Green tea catechins as a BACE1 (β-secretase) inhibitor. *Bioorg. Med. Chem. Lett.* **13**, 3905-3908
49. Obregon, D., Hou, H., Deng, J., Giunta, B., Tian, J., Darlington, D., Shahaduzzaman, M., Zhu, Y., Mori, T., Mattson, M.P., and Tan, J. (2012) Soluble amyloid precursor protein-α modulates β-secretase activity and amyloid-β generation. *Nat. Commun.* **3**, 777
50. Kaden, D., Munter, L. M., Joshi, M., Treiber, C., Weise, C., Bethge, T., Voigt, P., Schaefer, M., Beyermann, M., Reif, B., and Multhaup, G. (2008) Homophilic interactions of the amyloid precursor protein (APP) ectodomain are regulated by the loop region and affect β-secretase cleavage of APP. *J. Biol. Chem.* **283**, 7271-7279
51. Young-Pearse, T. L., Chen, A. C., Chang, R., Marquez, C., and Selkoe, D. J. (2008) Secreted APP regulates the function of full-length APP in neurite outgrowth through interaction with integrin β1. *Neural. Dev.* **3**, 15
52. Gralle, M., Botelho, M. G., and Wouters, F. S. (2009) Neuroprotective secreted amyloid precursor protein acts by disrupting amyloid precursor protein dimers. *J. Biol. Chem.* **284**, 15016-15025
53. Akiyama, H., Barger, S., Barnum, S., Bradt, B., Bauer, J., Cole, G. M., Cooper, N. R., Eikelenboom, P., Emmerling, M., Fiebich, B. L., Finch, C. E., Frautschy, S., Griffin, W. S., Hampel, H., Hull, M., *et al.* (2000) Inflammation and Alzheimer's disease. *Neurobiol. Aging* **21**, 383-421
54. Heneka, M. T., Carson, M. J., El Khoury, J., Landreth, G. E., Brosseron, F., Feinstein, D. L., Jacobs, A. H., Wyss-Coray, T., Vitorica, J., Ransohoff, R. M., Herrup, K., Frautschy, S. A., Finsen, B., Brown, G. C., Verkhratsky, A., *et al.* (2015) Neuroinflammation in Alzheimer's disease. *Lancet Neurol*. **14**, 388-405
55. Andreasson, K. I., Bachstetter, A. D., Colonna, M., Ginhoux, F., Holmes, C., Lamb, B., Landreth, G., Lee, D. C., Low, D., Lynch, M. A., Monsonego, A., O'Banion, M. K., Pekny, M., Puschmann, T., Russek-Blum, N., *et al.* (2016) Targeting innate immunity for neurodegenerative disorders of the central nervous system. *J. Neurochem.* **138**, 653-693
56. Valko, M., Leibfritz, D., Moncol, J., Cronin, M.T., Mazur, M., and Telser, J. (2007) Free radicals and antioxidants in normal physiological functions and human disease. *Int. J. Biochem. Cell Biol.* **39**, 44-84
57. Yan, S. D., Chen, X., Fu, J., Chen, M., Zhu, H., Roher, A., Slattery, T., Zhao, L., Nagashima, M., Morser, J., Migheli, A., Nawroth, P., Stern, D., and Schmidt, A. M. (1996) RAGE and amyloid-β peptide neurotoxicity in Alzheimer's disease. *Nature* **382**, 685-691
58. Markesbery, W. R. (1997) Oxidative stress hypothesis in Alzheimer's disease. *Free Radic. Biol. Med.* **23**, 134-147



Downloaded from http://www.jbc.org/ by guest on January 9, 2019

59. Selkoe, D. J. (2002) Alzheimer's disease is a synaptic failure. *Science* **298**, 789-791
60. Shankar, G.M., and Walsh, D.M. (2009) Alzheimer's disease: synaptic dysfunction and Aβ. *Mol. Neurodegener.* **4**, 48
61. Klyubin, I., Cullen, W. K., Hu, N. W., and Rowan, M. J. (2012) Alzheimer's disease Aβ assemblies mediating rapid disruption of synaptic plasticity and memory. *Mol. Brain* **5**, 25
62. Valtorta, F., Pennuto, M., Bonanomi, D., and Benfenati, F. (2004) Synaptophysin: leading actor or walk-on role in synaptic vesicle exocytosis? *BioEssays* **26**, 445-453
63. Reagan-Shaw, S., Nihal, M., and Ahmad, N. (2008) Dose translation from animal to human studies revisited. *FASEB J.* **22**, 659-661
64. Barnes, D. G., and Dourson, M. (1988) Reference dose (RfD): description and use in health risk assessments. *Regul. Toxicol. Pharmacol.* **8**, 471-486
65. Williamson, G.1., Dionisi, F., and Renouf, M. (2011) Flavanols from green tea and phenolic acids from coffee: critical quantitative evaluation of the pharmacokinetic data in humans after consumption of single doses of beverages. *Mol. Nutr. Food Res.* **55**, 864-873
66. Manach, C., Williamson, G., Morand, C., Scalbert, A., and Rémésy, C. (2005) Bioavailability and bioefficacy of polyphenols in humans. I. Review of 97 bioavailability studies. *Am. J. Clin. Nutr.* **81**, 230S-242S
67. Moore, R.J., Jackson, K.G., and Minihane, A.M. (2009) Green tea (*Camellia sinensis*) catechins and vascular function. *Br. J. Nutr.* **102**, 1790-1802
68. Ullmann, U., Haller, J., Decourt, J.P., Girault, N., Girault, J., Richard-Caudron, A.S., Pineau, B., and Weber, P. (2003) A single ascending dose study of epigallocatechin gallate in healthy volunteers. *J. Int. Med. Res.* **31**, 88-101
69. Yang, C., Tian, Y., Zhang, Z., Xu, F., and Chen, Y. (2007) High-performance liquid chromatography-electrospray ionization mass spectrometry determination of sodium ferulate in human plasma. *J. Pharm. Biomed. Anal.* **43**, 945-950
70. Kern, S.M., Bennett, R.N., Mellon, F.A., Kroon, P.A., and Garcia-Conesa, M.T. (2003) Absorption of hydroxycinnamates in humans after high-bran cereal consumption. *J. Agric. Food Chem.* **51**, 6050-6055
71. Bourne, L.C., and Rice-Evans, C. (1998) Bioavailability of ferulic acid. *Biochem. Biophys. Res. Commun.* **253**, 222-227
72. Gasperotti, M., Passamonti, S., Tramer, F., Masuero, D., Guella, G., Mattivi, F., and Vrhovsek, U. (2015) Fate of microbial metabolites of dietary polyphenols in rats: Is the brain their target destination? *ACS Chem. Neurosci.* **6**,1341-1352
73. Bertram, L., and Tanzi, R.E. (2012) The genetics of Alzheimer's disease. *Prog. Mol. Biol. Transl. Sci.* **107**, 79-100
74. Jankowsky, J. L., Slunt, H. H., Gonzales, V., Jenkins, N. A., Copeland, N. G., and Borchelt, D. R. (2004) APP processing and amyloid deposition in mice haplo-insufficient for presenilin 1. *Neurobiol. Aging* **25**, 885-892
75. De Rosa, R., Garcia, A.A., Braschi, C., Capsoni, S., Maffei, L., Berardi, N., and Cattaneo, A. (2005) Intranasal administration of nerve growth factor (NGF) rescues recognition memory deficits in AD11 anti-NGF transgenic mice. *Proc. Natl. Acad. Sci. U.S.A.* **102**, 3811-3816
76. Alamed, J., Wilcock, D.M., Diamond, D.M., Gordon, M.N., and Morgan, D. (2006) Two-day radial-arm water maze learning and memory task; robust resolution of amyloid-related memory deficits in transgenic mice. *Nat. Protoc.* **1**, 1671-1679




Downloaded from http://www.jbc.org/ by guest on January 9, 2019

77. Franklin, K. B. J., and Paxinos, G. (2001) *The Mouse Brain in Stereotaxic Coordinates*, Academic Press, San Diego
78. Kawarabayashi, T., Younkin, L.H., Saido, T.C., Shoji, M., Ashe, K.H., and Younkin, S.G. (2001) Age-dependent changes in brain, CSF, and plasma amyloid (β) protein in the Tg2576 transgenic mouse model of Alzheimer's disease. *J. Neurosci.* **21**, 372-381
79. Horikoshi, Y., Sakaguchi, G., Becker, A.G., Gray, A.J., Duff, K., Aisen, P.S., Yamaguchi, H., Maeda, M., Kinoshita, N., and Matsuoka, Y. (2004) Development of Aβ terminal end-specific antibodies and sensitive ELISA for Aβ variant. *Biochem. Biophys. Res. Commun.* **319**, 733-737
80. Xia, W., Yang, T., Shankar, G., Smith, I.M., Shen, Y., Walsh, D.M., and Selkoe, D.J. (2009) A specific enzyme-linked immunosorbent assay for measuring β-amyloid protein oligomers in human plasma and brain tissue of patients with Alzheimer disease. *Arch. Neurol.* **66**, 190-199
81. Monney, L., Sabatos, C. A., Gaglia, J. L., Ryu, A., Waldner, H., Chernova, T., Manning, S., Greenfield, E. A., Coyle, A. J., Sobel, R. A., Freeman, G. J., and Kuchroo, V. K. (2002) Th1-specific cell surface protein Tim-3 regulates macrophage activation and severity of an autoimmune disease. *Nature* **415**, 536-541

Downloaded from http://www.jbc.org/ by guest on January 9, 2019

**FOOTNOTES**

[1]To whom correspondence may be addressed: Depts. of Biomedical Sciences and Pathology, Saitama Medical Center and University, 1981 Kamoda, Kawagoe, Saitama 350-8550, Japan. Tel.: 81-49-228-3592; E-mail: t_mori@saitama-med.ac.jp.

[2]To whom correspondence may be addressed: Dept. of Physiology and Biophysics, Keck School of Medicine, University of Southern California, 1501 San Pablo St., Rm. 337, Los Angeles, CA 90089-2821. Tel.: 323-442-2492; E-mail: ttown@usc.edu.

[3]The abbreviations used are: AD, Alzheimer's disease; Aβ, amyloid β-protein; APP, amyloid β-protein precursor; sAPP-α, soluble APP-α; EGCG, (−)-epigallocatechin-3-gallate; FA, ferulic acid; ADAM10, a disintegrin and metalloproteinase domain-containing protein 10; APP/PS1, the mutant human amyloid β-protein precursor-presenilin 1; APP/PS1 mice, APP/PS1 transgenic mouse model of cerebral amyloidosis; RAWM, radial arm water maze; ANOVA, analysis of variance; RSC, retrosplenial cortex; EC, entorhinal cortex; H, hippocampus; ROI, regions of interest; CAA, cerebral amyloid angiopathy; sAPP-β, soluble APP-β; β-CTF/C99, β-carboxyl-terminal fragment; P-β-CTF/P-C99, phospho-β-CTF; BACE1, β-site APP-cleaving enzyme 1; pADAM10, precursor ADAM10; mADAM10, mature (active) ADAM10; QPCR, real-time polymerase chain reaction; SOD1, superoxide dismutase 1; GPx1, glutathione peroxidase 1; GFAP, glial fibrillary acidic protein; Iba1, ionized calcium-binding adapter molecule 1; IR, immunoreactivity; $LD_{50}$, lethal dose for 50%; $APP_{swe}$, "Swedish" $APP_{K595N/M596L}$.

Downloaded from http://www.jbc.org/ by guest on January 9, 2019

## FIGURE LEGENDS

**Figure 1. Reversal of transgene-associated behavioral impairment in APP/PS1-EGCG/FA mice.** Data were obtained from APP/PS1 mice that received vehicle (*APP/PS1-V*, *n* = 8), EGCG (*APP/PS1-EGCG*, *n* = 8), FA (*APP/PS1-FA*, *n* = 8), or EGCG plus FA (*APP/PS1-EGCG/FA*, *n* = 8) and also wild-type mice that received vehicle (*WT-V*, *n* = 8), EGCG (*WT-EGCG*, *n* = 8), FA (*WT-FA*, *n* = 8), or EGCG plus FA (*WT-EGCG/FA*, *n* = 8) for 3 months after initial behavioral testing at 12 months of age. Data for *A-D* are presented as standard deviations of the means. All mice were tested with a comprehensive behavioral battery at 15 months. *A*, recognition index (%) in the novel object recognition test is shown for training (*left*) and retention (*right*) phases. *B*, Y-maze test data are represented as total arm entries (*left*) and spontaneous alternation (*right*). Two-day radial arm water maze test data are shown with five blocks per day for errors (*C*, *left and right*) and for escape latency (*D*, *left and right*). Statistical comparisons for *A-D* are between-groups. *, $p < 0.05$ for APP/PS1-V *versus* the other treated mice; †, $p < 0.05$, ††, $p < 0.01$ for APP/PS1-EGCG/FA *versus* APP/PS1-EGCG or APP/PS1-FA mice.

**Figure 2. Combination therapy reduces β-amyloid plaques in APP/PS1 brains.** *A-D*, representative images were taken from APP/PS1 mice that received vehicle (*APP/PS1-V*), EGCG (*APP/PS1-EGCG*), FA (*APP/PS1-FA*), or EGCG plus FA (*APP/PS1-EGCG/FA*) for 3 months starting at 12 months of age (mouse age at sacrifice = 15 months). Immunohistochemistry using an $A\beta_{17-24}$ monoclonal antibody (*4G8*) reveals cerebral β-amyloid deposits. Brain regions shown include: retrosplenial cortex (RSC, *top*); hippocampus (H, *middle*); and entorhinal cortex (EC, *bottom*). Each *right* image is a higher magnification image from insets.

**Figure 3. Combined treatment with EGCG plus FA effectively attenuates cerebral parenchymal and vascular β-amyloid deposits and lowers Aβ levels.** *A-C*, quantitative image analysis of Aβ burden (%) from 4G8 immunostain is shown. *D-F*, morphometric analysis of cerebral parenchymal β-amyloid deposit size. Mean plaque size is shown from blind assignment to one of three mutually exclusive categories: small (< 25 μm; *D*), medium (between 25 and 50 μm; *E*), or large (> 50 μm; *F*). *G*, severity of cerebral amyloid angiopathy (mean CAA deposit number) is shown. For *A-C*, Each brain region is indicated on the *x* axis (RSC, H, and EC). For *D-F*, mean deposit number is shown on the *y* axis, and brain region is denoted on the *x* axis. For *G*, mean CAA number is shown on the *y* axis, and brain region is presented on the *x* axis. Data were obtained from APP/PS1 mice received to vehicle (*APP/PS1-V*, *n* = 8), EGCG (*APP/PS1-EGCG*, *n* = 8), FA (*APP/PS1-FA*, *n* = 8), or EGCG plus FA (*APP/PS1-EGCG/FA*, *n* = 8) for 3 months beginning at 12 months of age (mouse age at sacrifice = 15 months) for *A-G* in addition to 12-month-old APP/PS1-mice (*APP/PS1-12M, n* = 8) for *A-C*. Data for *A-G* are presented as standard deviations of the means. Statistical comparisons for *A-G* are between-groups within each brain region. *, $p < 0.05$; **, $p < 0.01$; ***, $p \leq 0.001$ for APP/PS1-V *versus* the other treated mice; †, $p < 0.05$; ††, $p < 0.01$ for APP/PS1-EGCG/FA *versus* APP/PS1-EGCG or APP/PS1-FA mice.

**Figure 4. Combination therapy with EGCG and FA significantly lowers Aβ levels.** *A*, TBS-soluble; *B*, detergent-soluble; and *C*, 5 M guanidine HCl-extractable fractions from brain homogenates were individually measured by sandwich ELISA for human $A\beta_{1-40}$ (*left*) and $A\beta_{1-42}$ (*right*). Data were obtained from APP/PS1 mice received to vehicle (*APP/PS1-V*, *n* = 8), EGCG (*APP/PS1-EGCG*, *n* = 8), FA (*APP/PS1-FA*, *n* = 8), or EGCG plus FA (*APP/PS1-EGCG/FA*, *n* = 8) for 3 months beginning at 12 months of age (mouse age at sacrifice = 15 months) for *A-C*. Data for *A-C* are presented as standard deviations of the means. Statistical comparisons for *A-C* are between-groups for each Aβ species. *, $p < 0.05$; **, $p < 0.01$; ***, $p \leq 0.001$ for APP/PS1-V *versus* the other treated mice; †, $p < 0.05$; ††, $p < 0.01$ for APP/PS1-EGCG/FA *versus* APP/PS1-EGCG or APP/PS1-FA mice.



Downloaded from http://www.jbc.org/ by guest on January 9, 2019

**Figure 5. Combined therapy promotes nonamyloidogenic and inhibits amyloidogenic APP cleavage.** Data were obtained from APP/PS1 mice that received vehicle (*APP/PS1-V*, *n* = 8), EGCG (*APP/PS1-EGCG*, *n* = 8), FA (*APP/PS1-FA*, *n* = 8), or EGCG plus FA (*APP/PS1-EGCG/FA*, *n* = 8) for 3 months starting at 12 months of age. Western blots included each mouse (*n* = 8 per group) and quantitative data were averaged. Ten μg of protein from each sample was equally loaded per lane. Data for *B-E* are presented as standard deviations of the means. *A*, Western blots are shown using amino-terminal APP polyclonal antibody (*pAb N-APP*), carboxyl-terminal anti-sAPP-β-sw monoclonal antibody (*mAb 6A1*), and sAPP-α monoclonal antibody (*mAb 2B3*). Western blots are also shown using amino-terminal amyloid-$\beta_{1\text{-}17}$ (*Aβ*) monoclonal antibody (*mAb 82E1*), which detects amyloidogenic APP cleavage fragments, including Aβ monomer and oligomers as well as phospho-C99 (*P-C99*) and nonphospho-C99 (*C99*). Actin is included as a loading control, and densitometry values are indicated below each lane. *B-D*, densitometry data are shown for ratios of sAPP-α or sAPP-β to APP as well as P-C99 or C-99 to actin. *E*, abundance of (N) 82E1 Aβ oligomers in the detergent-soluble brain homogenate fraction (measured by sandwich ELISA) are shown. Statistical comparisons for *B-C and E* are between-groups. Statistical comparisons for *D* are within each protein and between-groups. *B*, ***, $p < 0.001$ for APP/PS1-EGCG and APP/PS1-EGCG/FA mice *versus* APP/PS1-V and APP/PS1-FA mice; *C-E*, **, $p < 0.01$; ***, $p < 0.001$ for APP/PS1-V *versus* the other treated mice; ††, $p < 0.01$; †††, $p < 0.001$ for APP/PS1-EGCG/FA *versus* APP/PS1-EGCG or APP/PS1-FA mice.

**Figure 6. EGCG plus FA increases ADAM10 and decreases BACE1 expression.** Data were obtained from APP/PS1 mice that were given vehicle (*APP/PS1-V*, *n* = 8), EGCG (*APP/PS1-EGCG*, *n* = 8), FA (*APP/PS1-FA*, *n* = 8), or EGCG plus FA (*APP/PS1-EGCG/FA*, *n* = 8) for 3 months starting at 12 months of age. Western blots included each mouse (*n* = 8 per group) and quantitative data were averaged. Ten μg of protein from each sample was equally loaded per lane. Data for *B-D* are presented as standard deviations of the means. *A*, Western blots are shown using carboxyl-terminal ADAM10 (*α-secretase candidate*) polyclonal antibody (pAb ADAM10), and carboxyl-terminal BACE1 (*β-secretase*) polyclonal antibody (*pAb BACE1*). Actin is included as an internal loading control, and densitometry data are shown below each lane. *D*ensitometry results are shown for ratios of precursor ADAM10 (*pADAM10, B*) or mature ADAM10 (*mADAM10, C*) to actin. *D*, densitometry data are shown for ratios of BACE1 to actin. Statistical comparisons for *B-D* are between-groups. *B-C*, ***, $p < 0.001$ for APP/PS1-EGCG and APP/PS1-EGCG/FA *versus* APP/PS1-V and APP/PS1-FA mice; *D*, ***, $p < 0.001$ for APP/PS1-V *versus* the other treated mice; †††, $p < 0.001$ for APP/PS1-EGCG/FA *versus* APP/PS1-EGCG or APP/PS1-FA mice.

**Figure 7. Mitigated astrocytosis and microgliosis in APP/PS1-EGCG/FA mice.** *A-D*, representative images were obtained from APP/PS1 mice that received vehicle (*APP/PS1-V*), EGCG (*APP/PS1-EGCG*), FA (*APP/PS1-FA*), or EGCG plus FA (*APP/PS1-EGCG/FA*) for 3 months starting at 12 months of age (mouse age at sacrifice = 15 months). Immunohistochemistry for glial fibrillary acidic protein (*GFAP*) and ionized calcium-binding adapter molecule 1 (*Iba1*) reveals β-amyloid deposit-associated astrocytosis (*left images*) and microgliosis (*right images*). Brain regions shown include: RSC (*top*); H (*middle*); and EC (*bottom*).

**Figure 8. APP/PS1-EGCG/FA mice had ameliorated astrocytosis and microgliosis.** Quantitative image analyses for astrocytosis (*A-C*) or microgliosis (*D-F*) burden are shown. Each brain region is indicated on the *x* axis. Data were obtained from APP/PS1 mice that received vehicle (*APP/PS1-V*, *n* = 8), EGCG (*APP/PS1-EGCG*, *n* = 8), FA (*APP/PS1-FA*, *n* = 8), or EGCG plus FA (*APP/PS1-EGCG/FA*, *n* = 8) for 3 months commencing at 12 months of age (mouse age at sacrifice = 15 months). Data for *A-F* are presented as standard deviations of the means. Statistical comparisons for *A-F* are within each brain region and between-groups. ***, $p \leq 0.001$ for APP/PS1-V *versus* the other treated mice; †, $p < 0.05$; ††, $p < 0.01$



Downloaded from http://www.jbc.org/ by guest on January 9, 2019

for APP/PS1-EGCG/FA *versus* APP/PS1-EGCG or APP/PS1-FA mice.

**Figure 9. Combination therapy with EGCG plus FA dampens neuroinflammation and oxidative stress.** Data were obtained from APP/PS1 mice that received vehicle (*APP/PS1-V*, *n* = 8), EGCG (*APP/PS1-EGCG*, *n* = 8), FA (*APP/PS1-FA*, *n* = 8), or EGCG plus FA (*APP/PS1-EGCG/FA*, *n* = 8) for 3 months commencing at 12 months of age (mouse age at sacrifice = 15 months). Data for *A-B* additionally included wild-type mice treated in parallel with vehicle (*WT-V*, *n* = 8), EGCG (*WT-EGCG*, *n* = 8), FA (*WT-FA*, *n* = 8), or EGCG plus FA (*WT-EGCG/FA*, *n* = 8). Data for *A-B* and *D-E* are presented as standard deviations of the means. QPCR for *A*, tumor necrosis factor-α (*TNF-α*) or interleukin-1β (*IL-1β*) proinflammatory cytokines or *B*, key oxidative stress markers superoxide dismutase 1 (*SOD1*) or glutathione peroxidase 1 (*GPx1*). Data for *A-B* are expressed as relative fold over WT-V mice. *C*, Western blots are shown using anti-Cu/Zn SOD polyclonal antibody (*pAb SOD1*) or by anti-GPx1 polyclonal antibody (*pAb GPx1*). Western blots included each mouse (*n* = 8 per group) and quantitative data were averaged. Ten μg of protein from each sample was equally loaded per lane. Actin is included as a loading control for each appropriate blot, and densitometry data are shown below each lane. Densitometry data are shown for ratios of SOD1 (*D*) to actin or for GPx1 (*E*) to actin. Statistical comparisons for *A-B* are between-groups but within each mRNA species. Statistical comparisons for *D-E* are within each protein and between-groups. *, $p < 0.05$; **, $p < 0.01$; ***, $p < 0.001$ for APP/PS1-V *versus* the other treated mice; †, $p < 0.05$; †††, $p < 0.001$ for APP/PS1-EGCG/FA *versus* APP/PS1-EGCG or APP/PS1-FA mice.

**Figure 10. Synaptotoxicity in APP/PS1 mice is attenuated by EGCG plus FA combination treatment.** Data were obtained from PSAPP mice treated with vehicle (*APP/PS1-V*, *n* = 8), OG (*APP/PS1-EGCG*, *n* = 8), FA (*APP/PS1-FA*, *n* = 8), or EGCG plus FA (*APP/PS1-EGCG/FA*, *n* = 8) for 3 months commencing at 12 months of age (mouse age at sacrifice = 15 months). Data for *E-F* are presented as standard deviations of the means. *A-D*, immunohistochemistry using a carboxyl-terminal synaptophysin monoclonal antibody. Brain regions shown include: CA1 (*left*) and EC (*right*). *E-F*, quantitative image analyses for synaptophysin immunoreactivity (IR) are shown. Brain region is indicated on the *x* axis. Statistical comparisons for *E-F* are within each brain region and between-groups. ***, $p < 0.001$ for APP/PS1-V *versus* the other treated mice; †, $p < 0.05$ for APP/PS1-EGCG/FA *versus* APP/PS1-EGCG or APP/PS1-FA mice.

Downloaded from http://www.jbc.org/ by guest on January 9, 2019

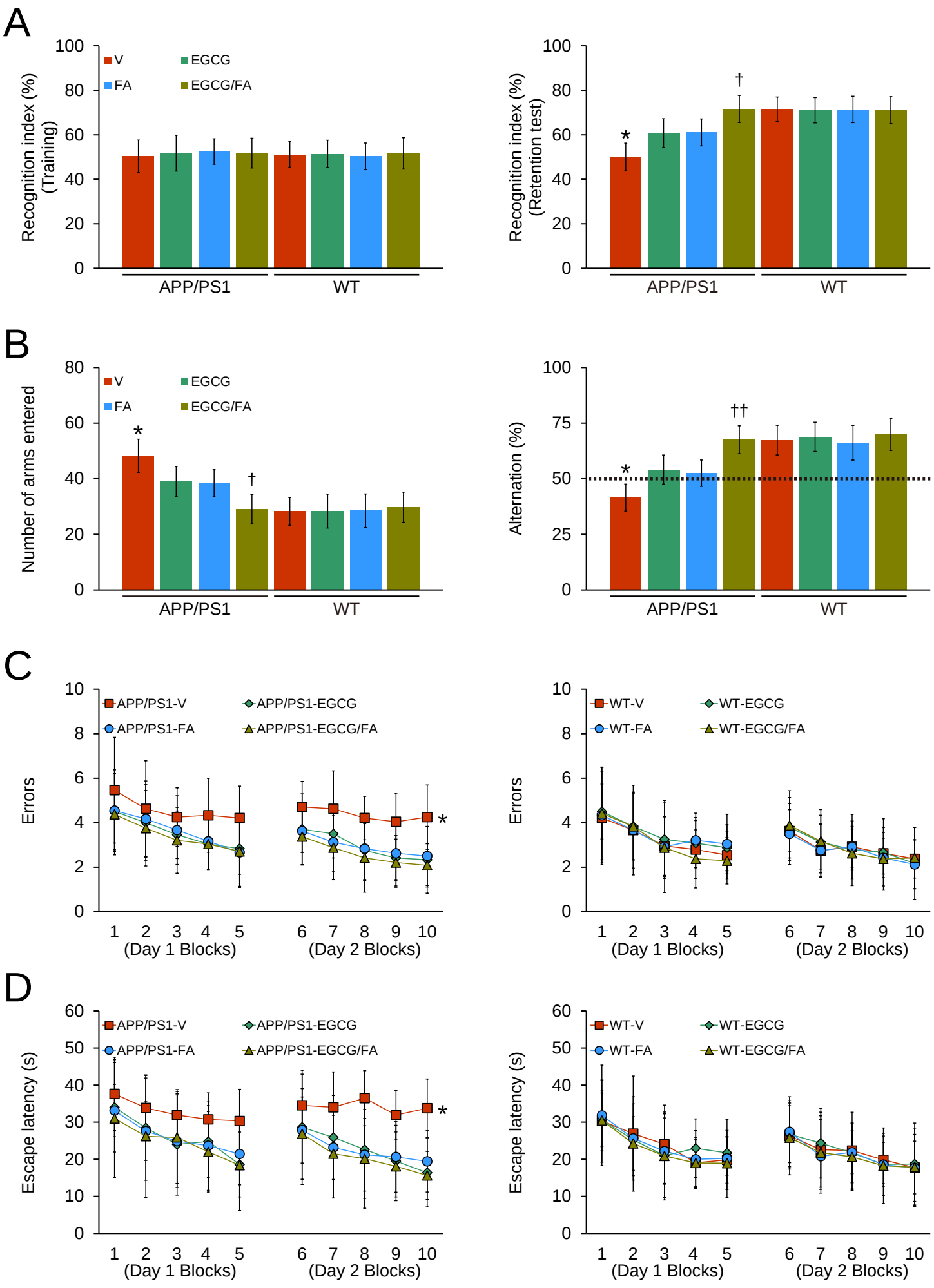


Figure 1A-D

Downloaded from http://www.jbc.org/ by guest on January 9, 2019

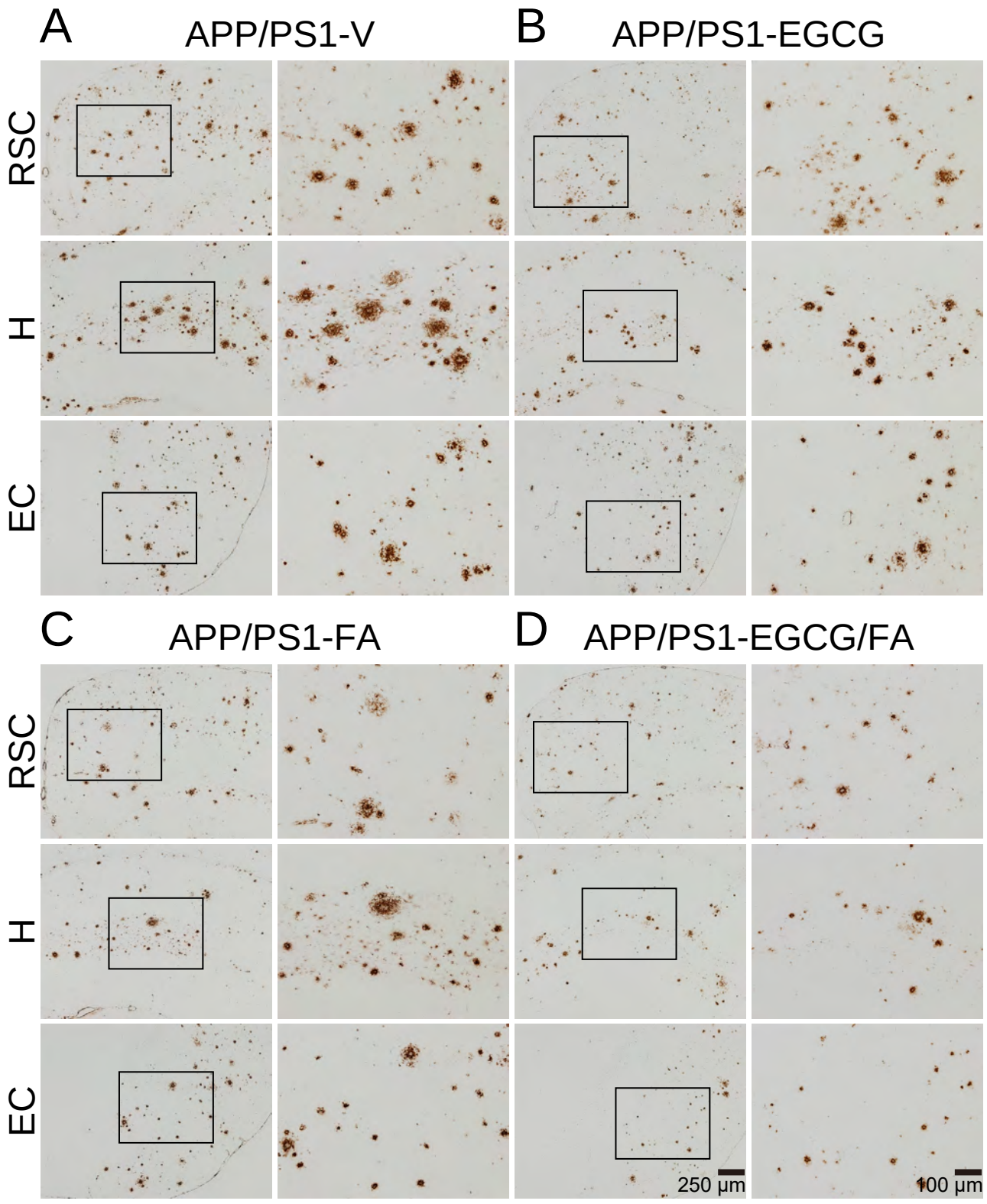


Figure 2A-D

Downloaded from http://www.jbc.org/ by guest on January 9, 2019

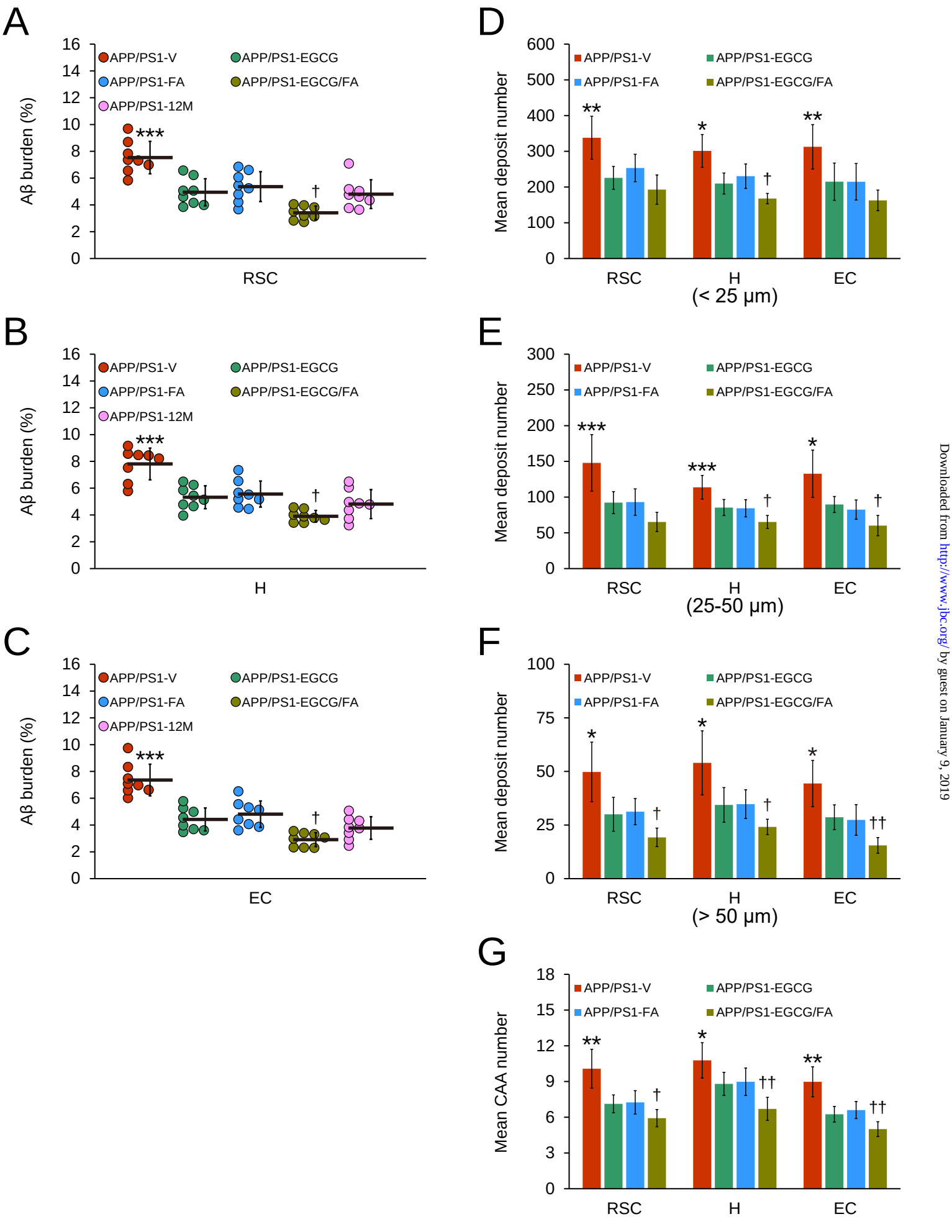


Downloaded from http://www.jbc.org/ by guest on January 9, 2019

Figure 3A-G

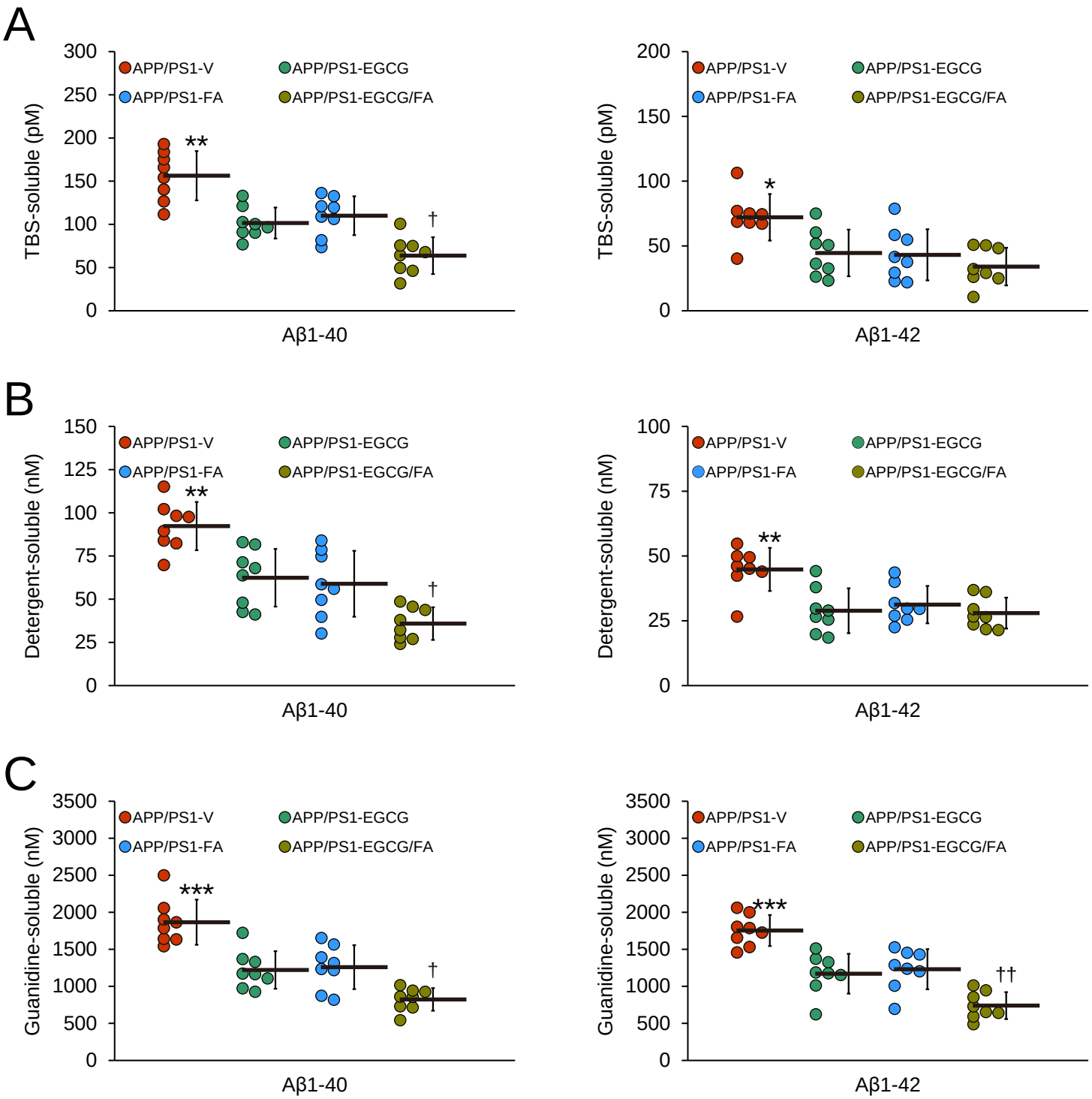


Figure 4A-C

Downloaded from http://www.jbc.org/ by guest on January 9, 2019

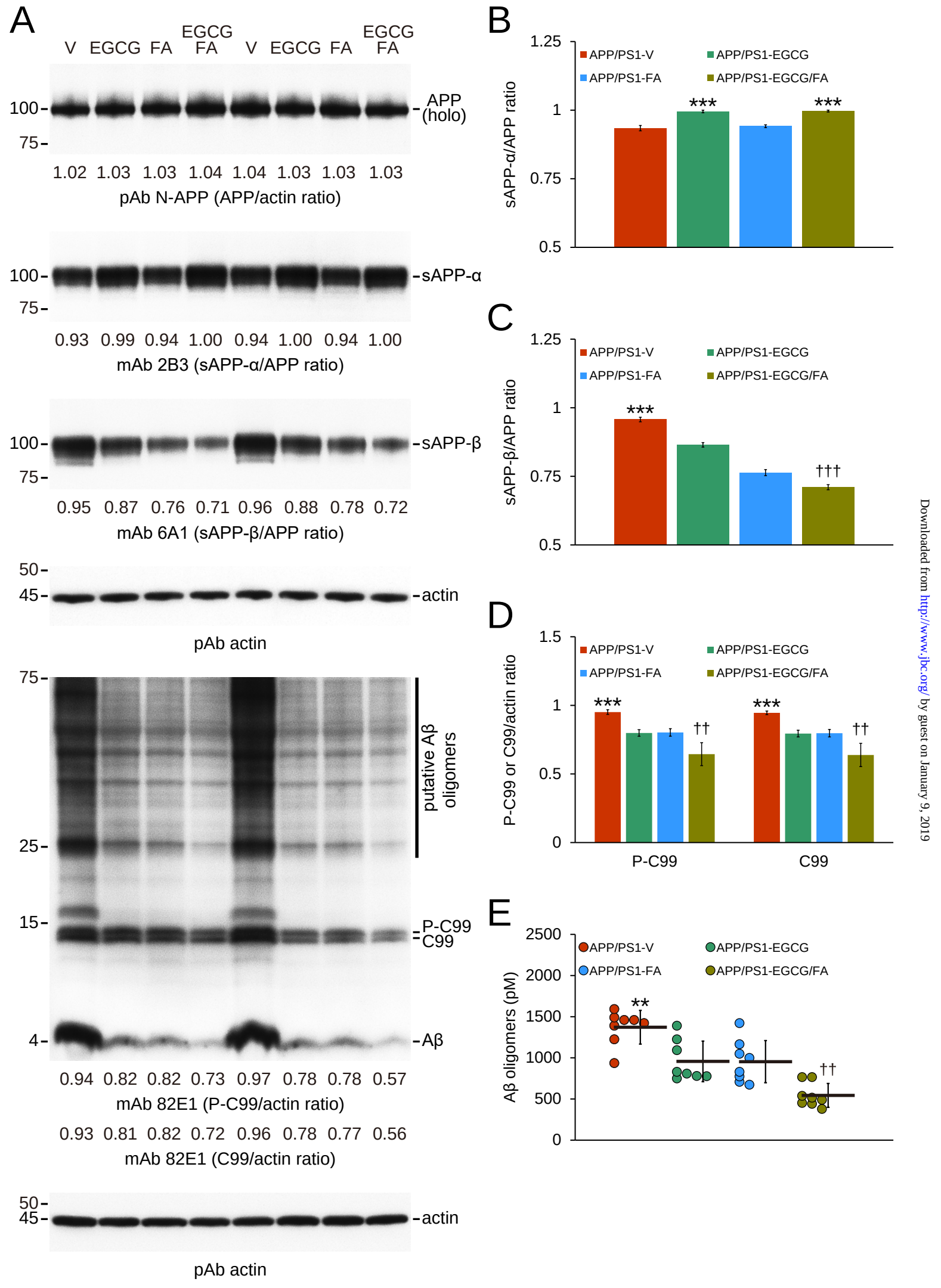


Figure 5A-E

Downloaded from http://www.jbc.org/ by guest on January 9, 2019

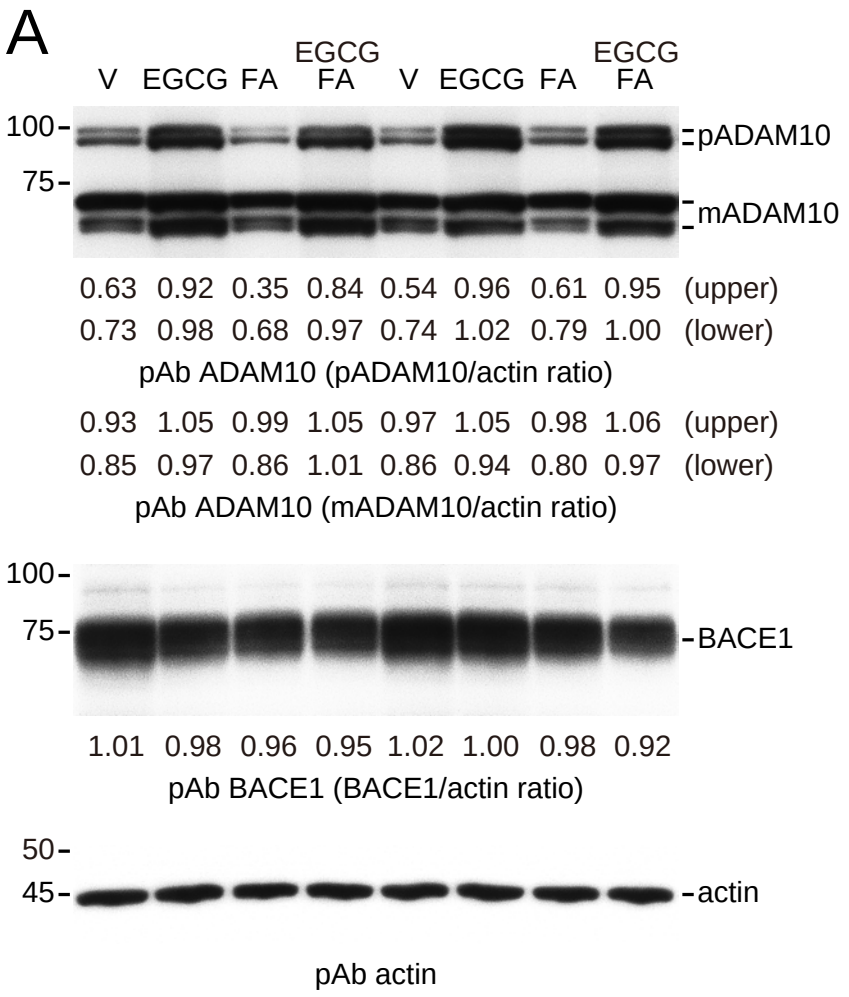


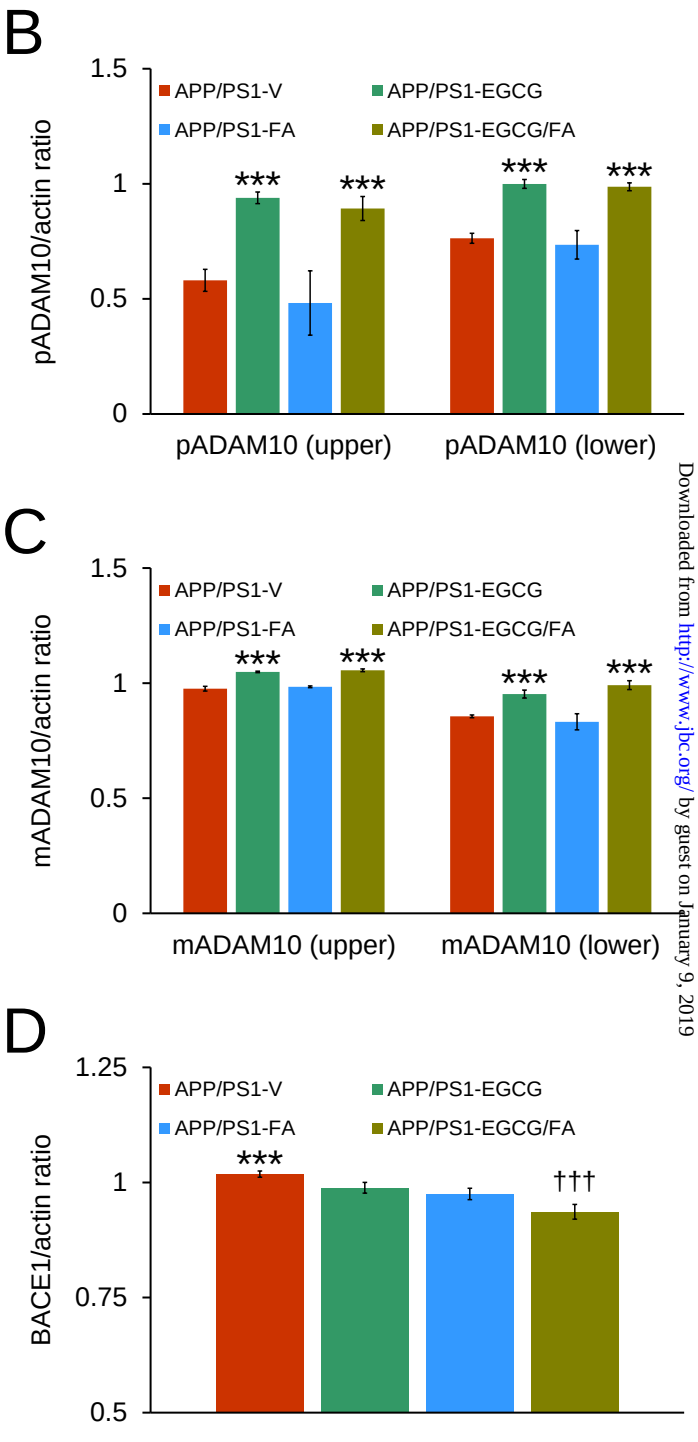


Downloaded from http://www.jbc.org/ by guest on January 9, 2019

Figure 6A-D

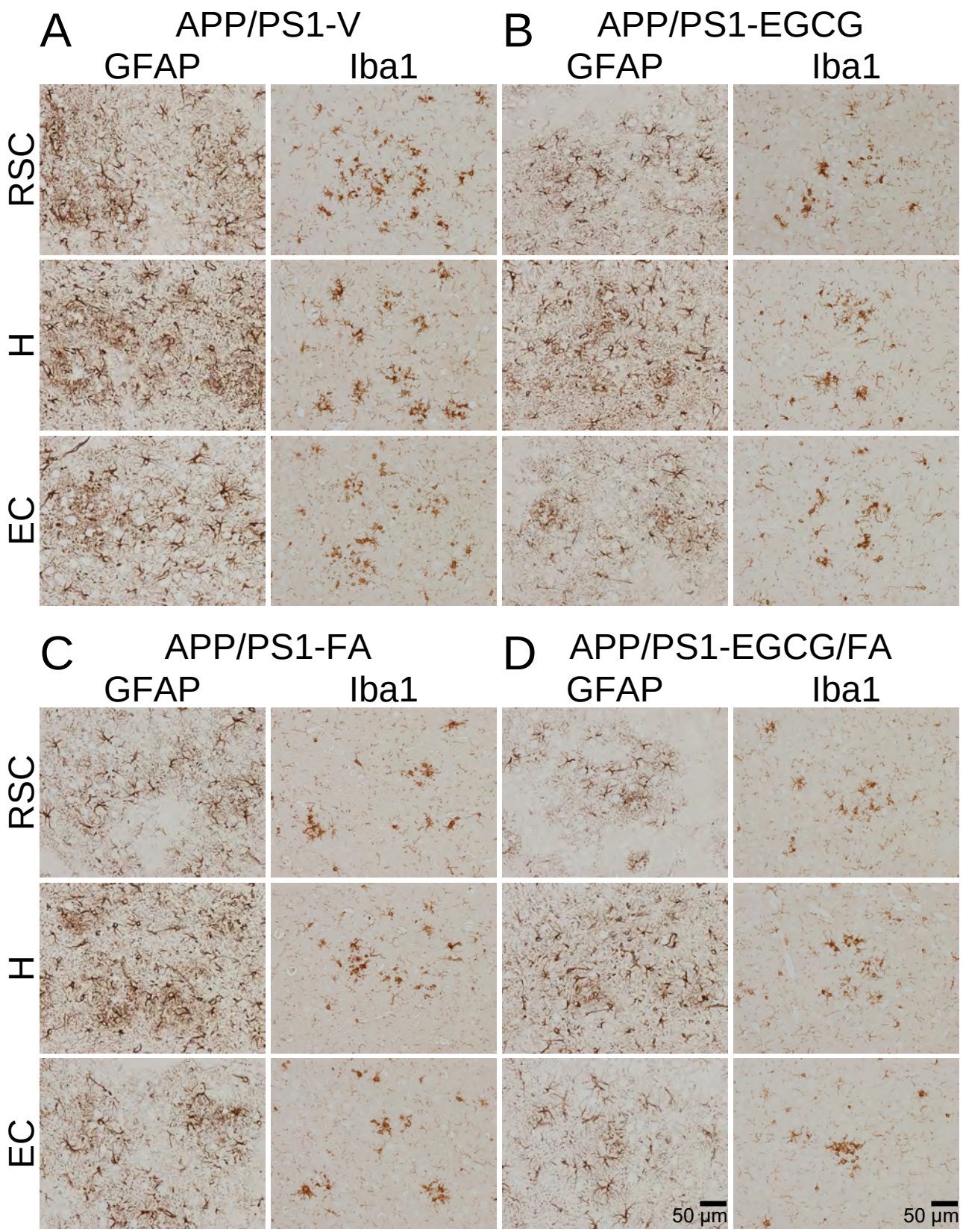


Figure 7A-D

Downloaded from http://www.jbc.org/ by guest on January 9, 2019

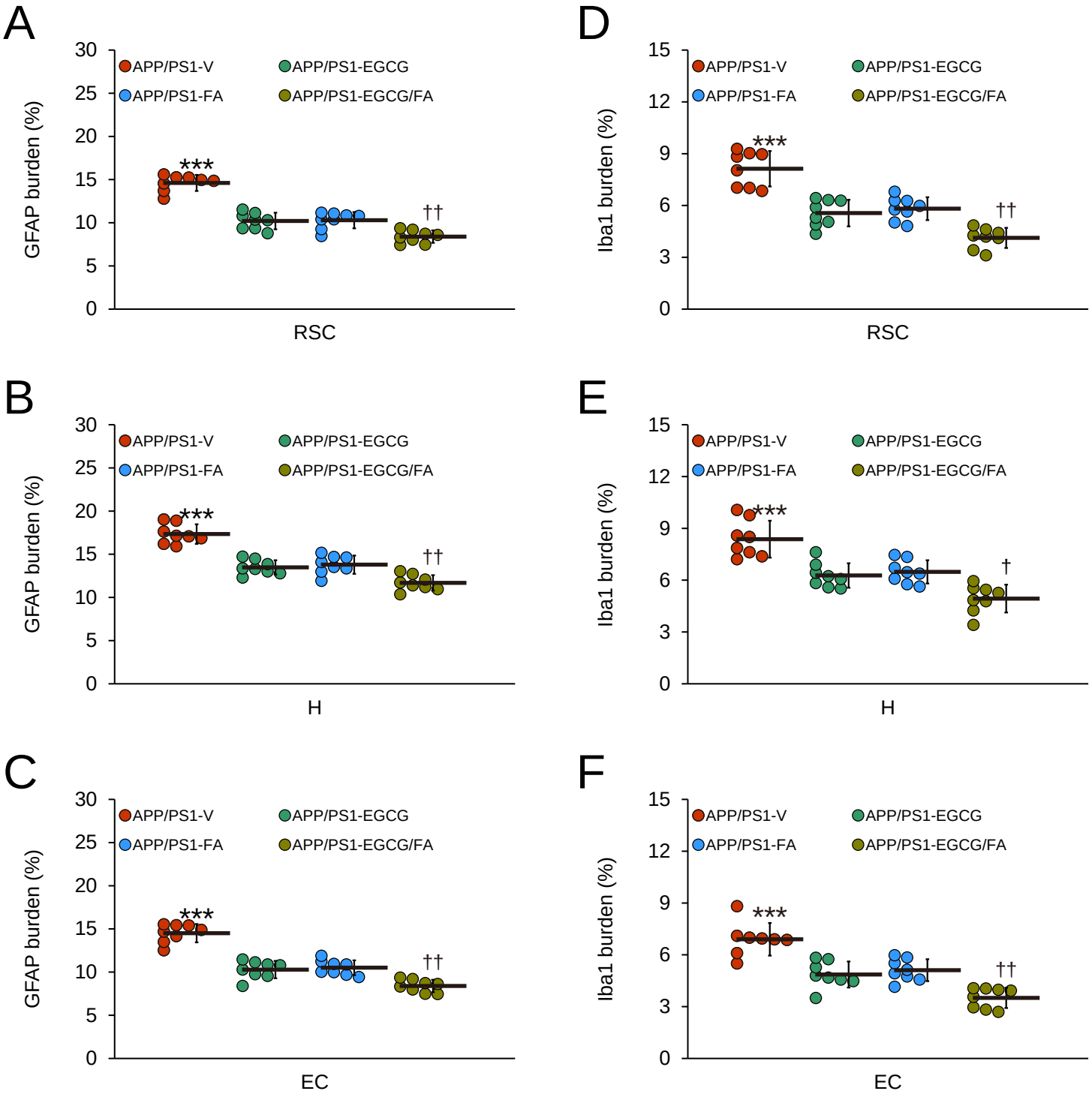


Figure 8A-F

Downloaded from http://www.jbc.org/ by guest on January 9, 2019

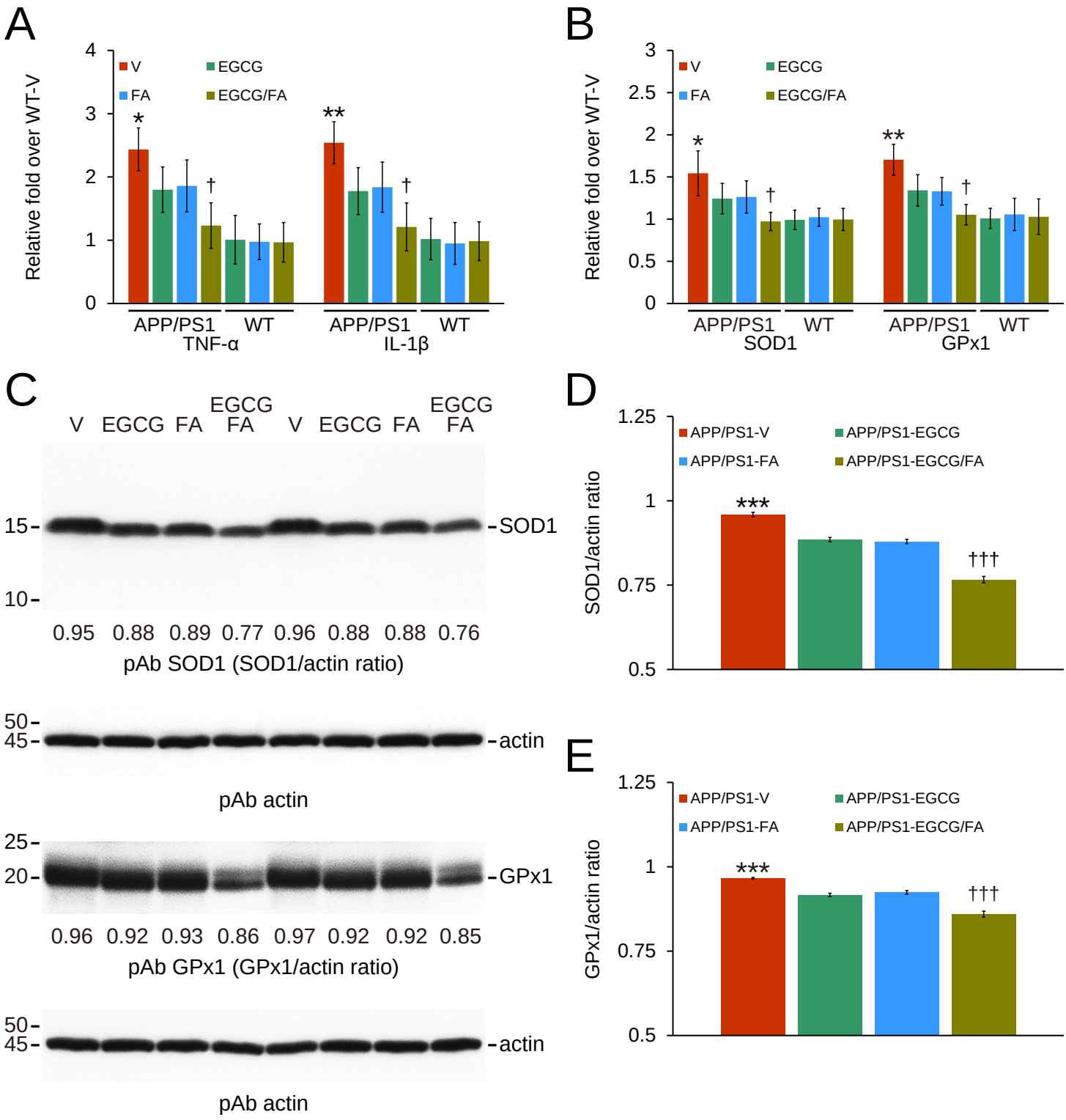


Figure 9A-E

Downloaded from http://www.jbc.org/ by guest on January 9, 2019

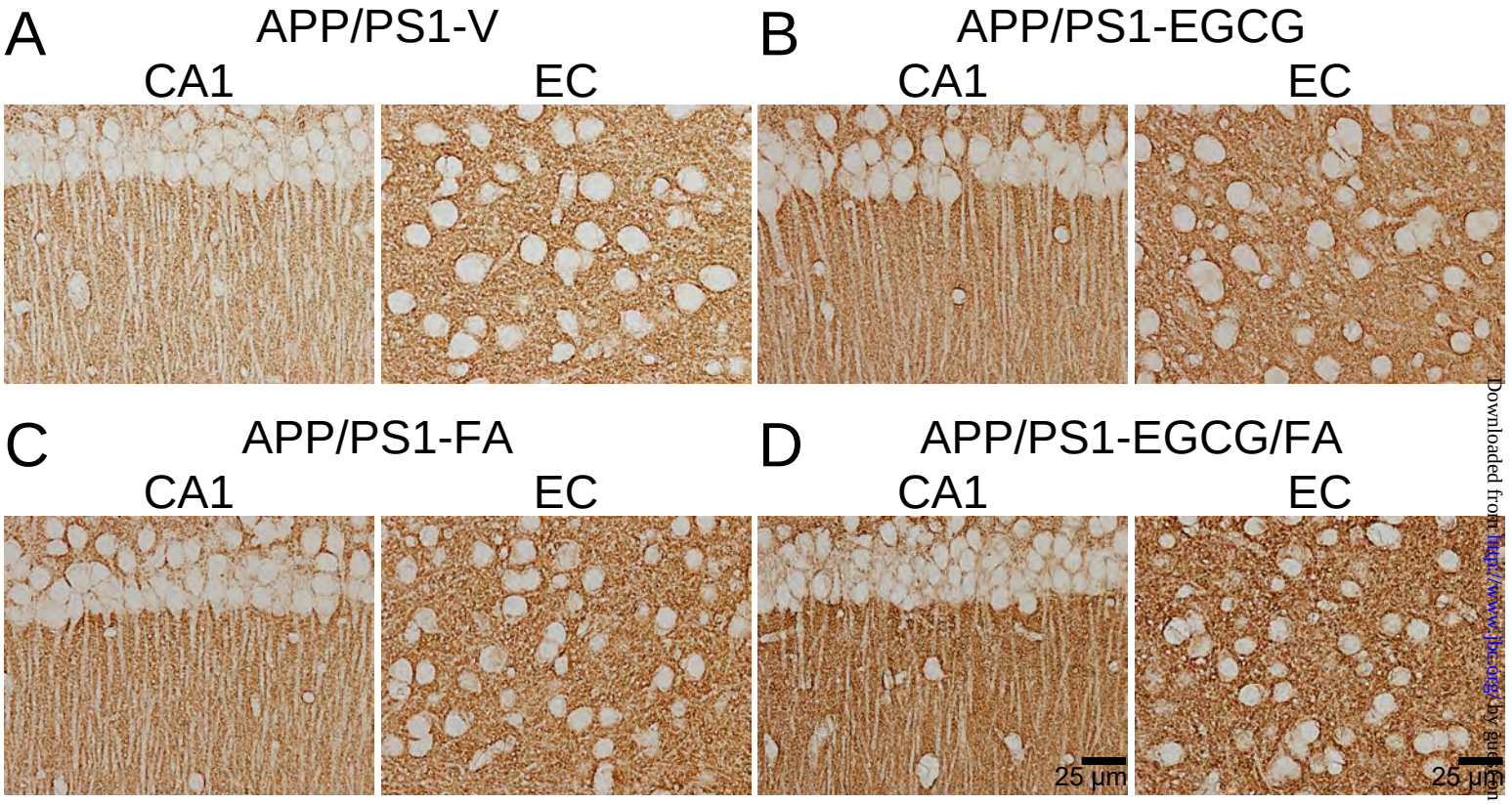


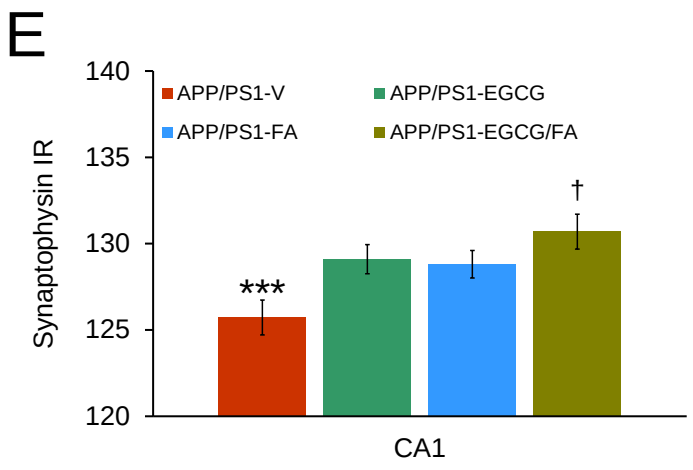


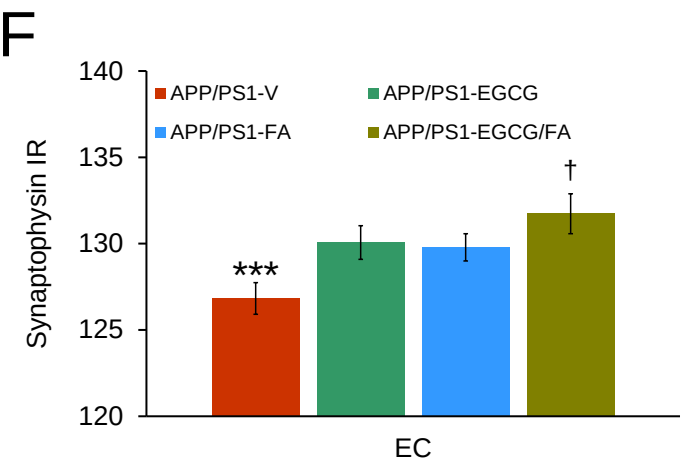


Downloaded from http://www.jbc.org/ by guest on January 9, 2019

Figure 10A-F

**Combined treatment with the phenolics (−)-epigallocatechin-3-gallate and ferulic acid improves cognition and reduces Alzheimer-like pathology in mice**

Takashi Mori, Naoki Koyama, Jun Tan, Tatsuya Segawa, Masahiro Maeda and Terrence Town

*J. Biol. Chem. published online December 18, 2018*

Access the most updated version of this article at doi: 10.1074/jbc.RA118.004280

Alerts:
- When this article is cited
- When a correction for this article is posted

Click here to choose from all of JBC's e-mail alerts

Downloaded from http://www.jbc.org/ by guest on January 9, 2019